植物生态学报 2022, **46** (10): 1167-1199
Chinese Journal of Plant Ecology
DOI: 10.17521/cjpe.2022.0233
http://www.plant-ecology.com

日光诱导叶绿素荧光遥感及其在陆地生态系统监测中的应用

吴霖升 张永光* 章钊颖 张小康 吴云飞

南京大学国际地球系统科学研究所, 南京大学地理与海洋科学学院, 自然资源部国土卫星遥感应用重点实验室, 江苏省地理信息技术重点实验室, 南京, 210023

摘 要 日光诱导叶绿素荧光(SIF)是近十年来迅速发展的新型植被遥感技术, 可以弥补以“绿度”为基础的植被指数等传统光学遥感观测的不足, 为大尺度植被光合作用监测提供了新方法。随着塔基、无人机、机载和星载SIF观测技术的快速发展以及SIF机理研究的推进, SIF遥感为陆地生态系统生理生化参数和生产力反演、非生物胁迫早期探测、光合物候提取和植被蒸腾作用监测等研究提供了重要技术支撑。该文首先系统阐述了SIF遥感的基本原理、观测技术和反演算法, 进而回顾了SIF遥感在陆地生态系统监测中的应用现状, 最后对天空地一体化SIF观测、SIF机理研究、新兴生态学应用等领域进行展望。

关键词 日光诱导叶绿素荧光; 陆地生态系统; 光合作用; 非生物胁迫; 物候; 蒸腾作用

吴霖升, 张永光, 章钊颖, 张小康, 吴云飞 (2022). 日光诱导叶绿素荧光遥感及其在陆地生态系统监测中的应用. 植物生态学报, 46, 1167-1199. DOI: 10.17521/cjpe.2022.0233

Remote sensing of solar-induced chlorophyll fluorescence and its applications in terrestrial ecosystem monitoring

WU Lin-Sheng, ZHANG Yong-Guang*, ZHANG Zhao-Ying, ZHANG Xiao-Kang, and WU Yun-Fei

International Institute for Earth System Sciences, School of Geography and Ocean Science, Key Laboratory for Land Satellite Remote Sensing Applications of Ministry of Natural Resources, Jiangsu Provincial Key Laboratory of Geographic Information Science and Technology, Nanjing University, Nanjing 210023, China

Abstract

Recent advances in solar-induced chlorophyll fluorescence (SIF), which is a complement to optical remote sensing based on greenness observation, have made it possible to monitor the photosynthesis of plants in terrestrial ecosystems using state-of-the-art technologies. With the rapid development of tower-based, unmanned aerial vehicle (UAV), airborne and space-borne SIF observation technology and improving understanding of SIF mechanism, SIF is providing essential data support and mechanism understanding for the estimation of biological traits and gross primary production of terrestrial ecosystem, early detection of abiotic stress, extraction of photosynthetic phenology and monitoring of transpiration. In this review, we first introduce the fundamental theory, the observation systems and technologies and the retrieval method of SIF. Then, we review the applications of SIF in terrestrial ecosystem monitoring. Finally, we propose a roadmap of activities to facilitate future directions and discuss critical emerging applications of SIF in terrestrial ecosystem monitoring that can benefit from cross-disciplinary expertise.

Key words solar-induced chlorophyll fluorescence (SIF); terrestrial ecosystem; photosynthesis; abiotic stress; phenology; transpiration

Wu LS, Zhang YG, Zhang ZY, Zhang XK, Wu YF (2022). Remote sensing of solar-induced chlorophyll fluorescence and its applications in terrestrial ecosystem monitoring. *Chinese Journal of Plant Ecology*, 46, 1167-1199. DOI: 10.17521/cjpe.2022.0233

陆地生态系统通过植物光合作用吸收大气中大量的CO_2, 对陆地生态系统碳汇有重要的影响, 是目前较为经济可行和环境友好的减缓大气CO_2浓度升高的重要途径(Wang *et al*., 2020)。因此, 准确监测植被光合作用对陆地生态系统碳水循环过程的研究至关重要。遥感观测能够提供大尺度且时空连续的

收稿日期Received: 2022-06-06 接受日期Accepted: 2022-09-05
基金项目: 国家自然科学基金(42125105和42071388)。Supported by the National Natural Science Foundation of China (42125105 and 42071388).
* 通信作者Corresponding author (yongguang_zhang@nju.edu.cn)

植被变化信息, 是监测陆地生态系统不可或缺的技术手段(张扬建等, 2017; 刘良云等, 2022; Zeng *et al*., 2022b)。

近十年来, 日光诱导叶绿素荧光(solar-induced chlorophyll fluorescence, SIF)遥感具有直接探测植被光合作用的优势, 成为植被遥感领域最具突破性的研究前沿之一, 为陆地生态系统监测提供了新思路和新手段(章钊颖等, 2019; 秦其明等, 2020)。叶绿素荧光是植物进行光合作用过程中由光系统反应中心激发出来的光谱信号(Baker, 2008)。按激发光源和探测方式的不同, 叶绿素荧光的观测可以分为主动和被动两种观测技术, 其中SIF是在太阳光下, 由超高光谱遥感传感器观测植被上行光谱并在荧光波段范围内反演出的光信号, 属于被动观测技术(Porcar-Castell *et al*., 2014)。SIF技术突破了传统主动荧光观测的空间尺度瓶颈, 实现了从叶片、冠层到全球尺度的植物光合作用观测(Porcar-Castell *et al*., 2021)。如图1所示, 在生态学、地理学、遥感科学和大气科学等多学科融合的基础上, 随着近地面、机载和卫星SIF遥感数据的丰富以及SIF机理研究的推进, SIF遥感技术目前已被广泛应用于精确估算生态系统过程中的关键生理生化参数、植被总初级生产力(GPP)和及时监测植物胁迫、物候和蒸腾作用等生态系统过程。

自然保护地作为陆地生态系统重要的一部分, 是生态文明建设的核心载体之一(黄宝荣等, 2018)。然而, 随着工业化和城镇化的快速发展, 人类活动形成的生境斑块破碎化对生物多样性造成极大威胁, 影响了我国自然保护地的健康发展(侯鹏等, 2017; 彭杨靖等, 2018)。目前, 以SIF观测技术为主的中国生态系统光谱观测研究网络(ChinaSpec)已经遍布全国, 20多个站点覆盖了农田、草地、亚热带森林、温带落叶林、常绿针叶林、红树林湿地、长江口湿地、鄱阳湖湿地、温带稀树草原、高寒草甸等生态系统和自然保护地(Zhang *et al*., 2021a)。SIF遥感技术已经开始为自然保护地建设、美丽中国建设等重大国家需求提供新技术支撑。

为了更好地挖掘SIF遥感在陆地生态系统和自

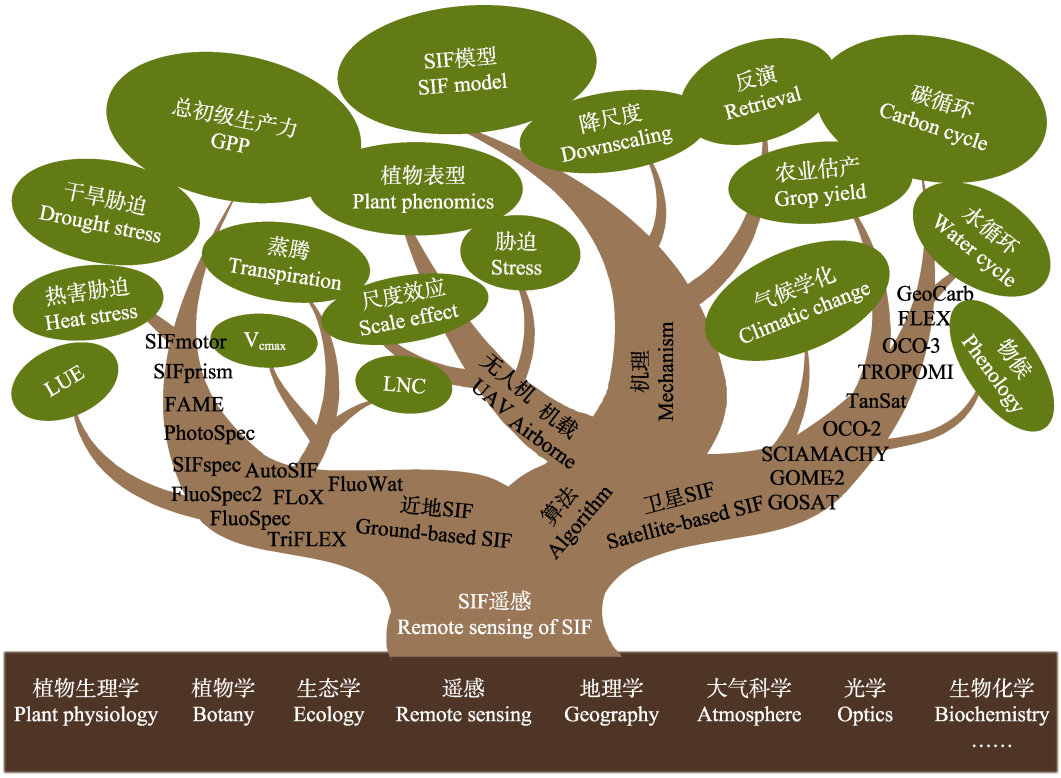

图1 日光诱导叶绿素荧光(SIF)遥感及在陆地生态系统监测中的应用现状概念图。LNC, 叶片氮含量; LUE, 光能利用率; V_{cmax}, 最大羧化速率。

Fig. 1 Remote sensing of solar-induced chlorophyll fluorescence (SIF) and its applications in terrestrial ecosystem monitoring. GPP, gross primary production; LNC, leaf nitrogen content; LUE, light use efficiency; V_{cmax}, the maximum rate of Rubisco carboxylation; UAV, unmanned aerial vehicle.

然保护地监测的潜力, 需要从多尺度SIF观测出发, 提取并解译SIF信号中的生理信息, 全面且定量地认识SIF与光合作用的关联机制及其在时空尺度上的变化特征(Mohammed *et al*., 2019; Porcar-Castell *et al*., 2021)。因此, 本文首先阐述了SIF遥感的基本原理、观测技术及反演方法, 然后回顾了SIF在陆地生态系统监测的几个主要应用方向, 最后对天空地一体化SIF观测、SIF机理研究、新兴生态学应用领域进行展望。

1 SIF遥感的基本原理、观测技术及反演算法

1.1 基本原理

叶绿素荧光是指叶绿素分子吸收光量子后, 激发态的叶绿素分子跃迁回基态的过程中发射的一种光谱信号(Meroni *et al*., 2009)。植物吸收的光能有3个去向: 光合作用、热耗散和叶绿素荧光, 三者在植物生理上密切关联。因此, 叶绿素荧光被誉为光合作用的“探针”, 在细胞和叶片尺度上已经被广泛应用于植物光合作用研究(Baker, 2008)。叶绿素荧光测量最初仅限于实验室内, 随着脉冲振幅调制(PAM)技术的发展, 逐渐走向野外测量, 促进了野外实地光合作用探测的研究, 并帮助阐明叶绿素荧光参数与CO_2同化之间的关系(Schreiber *et al*., 1986; Porcar-Castell *et al*., 2014)。然而, 由于PAM技术仅局限于叶片尺度, 其在冠层和景观尺度观测难度较大。为了填补这一空白, 叶绿素荧光研究出现新的发展趋势——尝试利用遥感平台实现区域及全球尺度叶绿素荧光观测。

SIF是叶绿素荧光研究的突破性进展, 实现了从遥感平台大尺度测量叶绿素荧光, 从而监测生态系统的光合作用动态(Ryu *et al*., 2019)。在日照下, 植物发射的叶绿素荧光仅占植物反射太阳辐射的1%至5%, 是非常微弱的光学信号(Grace *et al*., 2007)。由于太阳表层物质元素和地球大气对太阳光谱的吸收, 导致到达地表的太阳光谱有许多波段宽度为0.1至10 nm的暗线, 即夫琅禾费光谱线。当太阳光照射到植被并被反射出来时, 植被反射光在夫琅禾费吸收谱线波段也很微弱, 而植被发射的SIF可以对荧光波段的暗线进行一定的填充, 从而产生明显的反射峰(Meroni *et al*., 2009)。因此, SIF遥感探测原理就是计算来自植物的荧光辐射将暗线填充的程度(详细可见**1.3**反演算法介绍)。

1.2 观测技术

1.2.1 叶片及冠层尺度SIF观测

在叶片尺度, 借助FluoWat叶片夹可以获取全波段(650–800 nm)的SIF (Alonso *et al*., 2007)。在叶片夹顶部和底部的位置可以接入光纤, 同时借助一个滤波片, 过滤掉到达叶片超过650 nm的入射太阳光。此时, 光谱仪接收的波长位于650–800 nm之间的辐射亮度, 即为叶片激发的全波段SIF (图2)。在使用FluoWat叶片夹时, 可以通过叶片夹上的垂直定位十字星保持太阳-叶片-传感器之间的观测几何形状, 当太阳光照射在叶夹两侧的十字星中心, 即叶片夹出现明亮的光斑时, 可以进行测量。由于叶片夹的进光口较小(直径1 cm), 与太阳倾斜的角度稍有偏差, 叶片就会被叶片夹遮住。因此, 建议在每

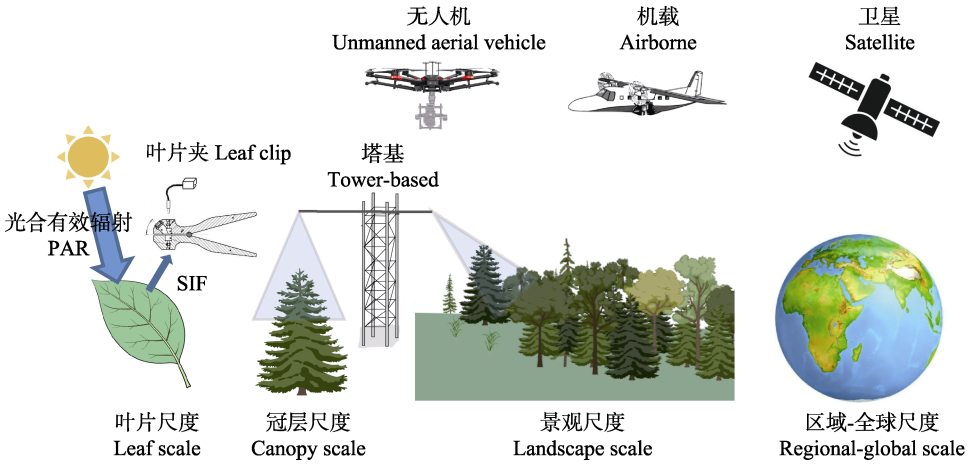

图2 多尺度下的多平台日光诱导叶绿素荧光(SIF)观测概念图。
Fig. 2 Illustration of solar-induced chlorophyll fluorescence (SIF) observation on multiple platforms at multiple scales. PAR, photosynthetically active radiation.

DOI: 10.17521/cjpe.2022.0233

组叶片测量前后均要测量入射光的辐射亮度, 以保证入射光的稳定性。

与叶片尺度相比, 地基(以塔基为主) SIF自动观测系统具有高频且连续的优点, 可以有效解决SIF的时间分辨率问题, 并且可以获取冠层尺度的SIF (图2)。如表1所示, 目前常用的塔基植被冠层SIF观测系统主要有FluoSpec (Yang *et al*., 2015), FloX (Julitta *et al*., 2017), FluoSpec2 (Yang *et al*., 2018b), PhotoSpec (Grossmann *et al*., 2018), FAME (Gu *et al*., 2019), SIFprism (Zhang *et al*., 2019c), SIFspec (Du *et al*., 2019), SIFmotor (Zhang *et al*., 2022b)等。这些塔基冠层SIF观测系统主要由1–3个光谱仪组成, 其中光谱分辨率较高的QEpro光谱仪(Ocean Optics, Dunedin, USA)主要用于SIF的反演, 而光谱分辨率较低的HR2000+或FLAME光谱仪(Ocean Optics, Dunedin, USA)主要用于植被反射率及植被指数的计算。塔基SIF观测系统方法及系统的详细介绍可见李朝晖等(2021)的综述。值得注意的是, 塔基冠层SIF观测系统的空间位置相对固定。因此在选择观测位置时应充分考虑观测目标的空间异质性, 以获取更具代表性的观测数据。此外, 由于从观测目标到传感器的辐射传输路径较短, 接收到的光谱几乎不受各种大气扰动(如尘埃颗粒、气溶胶、水蒸气等)的影响。因此在塔基测量中通常不进行大气校正。但是, Liu等(2019b)认为当观测塔的高度大于10 m时, 塔基观测的数据需要进行大气校正。

1.2.2 无人机及机载SIF观测

近年来, 搭载各种传感器的无人机和机载观测系统成为生态系统监测的有效工具(图2)。无人机观测系统的飞行参数(如高度、速度和观测角度等)可以根据观测需要进行灵活调整, 因此能够有效弥补地基观测的空间位置固定的问题, 也能够弥合地面和卫星观测之间的尺度差异(Atherton *et al*., 2018)。如表2所示, 无人机非成像SIF观测系统(Piccolo Doppio、HyUAS、AirSIF、FAME-UAV和FluorSpec)设计的基本思路与塔基SIF观测系统基本一致, 由一个亚纳米光谱分辨率的QEpro或者再加一个FLAME光谱仪组成。然而, 与塔基系统不同的是, 无人机SIF观测系统需要精确定位测量的地理位置, 除了使用无人机上的GPS, 还可以搭载一台RGB相机, 用于获取观测地物的位置。以搭载在六旋翼的经纬M600 Pro无人机上的SIF观测系统(Piccolo

表1 地基日光诱导叶绿素荧光(SIF)观测系统
Table 1 Ground-based solar-induced chlorophyll fluorescence (SIF) observation systems

观测系统 Observation system	光谱仪 Spectrometer	波段范围 Band range (nm)	光谱分辨率 Spectral resolution (nm)	SIF波段 SIF bands (nm)	参考文献 Reference
TriFLEX	HR2000+	630–815	0.50	687, 760	Daumard *et al*., 2010
	HR2000+	630–815	0.50		
	HR2000+	300–900	2.00		
SpectroFLEX	HR2000+	630–820	0.20	687, 760	Fournier *et al*., 2012
SFLUOR	HR4000	700–800	0.10	760	Cogliati *et al*., 2015a
	HR4000	400–1 000	1.00		
FluoSpec	HR2000+	680–775	0.13	760	Yang *et al*., 2015
SIF-Sys	STS-VIS	337–823	3.00	760	Burkart *et al*., 2015
FloX	QEpro	650–800	0.30	687, 760	Julitta *et al*., 2017
	FLAME-S	400–1 000	1.50		
FluoSpec2	QEpro	730–780	0.17	760	Yang *et al*., 2018b
	HR2000+	350–1 100	1.10		
AutoSIF	QE65pro	645–805	0.30	687, 760	Hu *et al*., 2018
PhotoSpec	QEpro 1	670–732	0.30	680–686, 745–758	Grossmann *et al*., 2018
	QEpro 2	729–784	0.30		
	FLAME	177–874	1.20		
FAME	QEpro	730–786	0.15	760	Gu *et al*., 2019
SIFspec	QE65pro	649–805	0.30	687, 760	Du *et al*., 2019
SIFprism	QEpro	650–800	0.30	687, 760	Zhang *et al*., 2019c
SIFmotor	QEpro	650–800	0.30	687, 760	Zhang *et al*., 2022b

表2 无人机(UAV)和机载日光诱导叶绿素荧光(SIF)观测系统
Table 2 Unmanned aerial vehicle (UAV) and airborne-based solar-induced chlorophyll fluorescence (SIF) observation systems

观测系统 Observation system	光谱仪 Spectrometer	波段范围 Band range (nm)	光谱分辨率 Spectral resolution (nm)	搭载平台 Platform	成像或非成像 Imaging or non-imaging	参考文献 Reference
Piccolo Doppio	QEpro	650–800	0.31	UAV	非成像 Non-imaging	MacArthur *et al*., 2014
	FLAME	400–950	1.30			
HyUAS	USB4000	350–1 000	1.50	UAV	非成像 Non-imaging	Garzonio *et al*., 2017
AirSIF	QEpro	498–877	0.80	UAV	非成像 Non-imaging	Bendig *et al*., 2020
FAME-UAV	QEpro	730–784	0.15	UAV	非成像 Non-imaging	Chang *et al*., 2020
	FLAME	350–1 000	1.30			
FluorSpec	QEpro	630–800	0.30	UAV	非成像 Non-imaging	Wang *et al*., 2021
CASI	CASI	408–947	7.50	机载 Airborne	成像 Imaging	Zarco-Tajeda *et al*., 2003
ROSIS	ROSIS	430–860	~7.00	机载 Airborne	成像 Imaging	Maier *et al*., 2004
AISA	AISA	520–884	1.60	机载 Airborne	成像 Imaging	Corp *et al*., 2006
AIRFLEX	AIRFLEX	687.3	0.50	机载 Airborne	非成像 Non-imaging	Moya *et al*., 2006
		760.7	1.00			
MCA-6	MCA-6	757.42	1.60	UAV	成像 Imaging	Zarco-Tejada *et al*., 2009
		760.47	1.57			
Micro-Hyperspec	VNIR	400–885	6.40	UAV	成像 Imaging	Zarco-Tejada *et al*., 2012
APEX	APEX	400–2 500	5.70	机载 Airborne	成像 Imaging	Damm *et al*., 2015
HyPlant	FLUO	670–800	0.25	机载 Airborne	成像 Imaging	Rascher *et al*., 2015
	DUAL	370–2 500	3.00/10.00			
AisaEAGLE	AisaEAGLE	400–970	3.30	飞艇 Airship	成像 Imaging	Ni *et al*., 2016
CFIS	CSIF	737–772	<0.10	机载 Airborne	成像 Imaging	Frankenberg *et al*., 2018
Nano-Hyperspec	VNIR	400–1 000	6.00	UAV	成像 Imaging	Wu *et al*., 2022a
FIREFLY	Fluorescence	670–780	0.10–0.20	机载 Airborne	成像 Imaging	Paynter *et al*., 2020
VNIR E-Series	VNIR	400–1 000	5.80	机载 Airborne	成像 Imaging	Belwalkar *et al*., 2022

Doppio)为例, 已有观测结果表明该系统能提供准确的冠层SIF和反射率数据(Zhang *et al*., 2022a)。然而, 无人机SIF观测系统的研发与应用仍处于早期阶段, 主要围绕无人机系统与地面观测系统观测的一致性(Garzonio *et al*., 2017), 无人机系统足迹范围(Gautam *et al*., 2020), 农作物的SIF观测(Chang *et al*., 2020; Wang *et al*., 2021), 无人机系统影响因素(Bendig *et al*., 2020)和植被覆盖度对SIF信号的影响(Zhang *et al*., 2022a)等方面进行研究。基于无人机平台的SIF观测仍存在一些难点, 如传感器和观测目标之间存在一定距离, 大气散射和程辐射会影响基于无人机平台的冠层SIF反演。因此, 基于无人机平台的冠层SIF观测系统需要更精确的大气校正算法, 或者能够消除大气影响的SIF反演算法, 以进一步提高SIF反演精度。

机载和无人机成像高光谱观测已被尝试用于SIF反演。例如CASI、ROSIS、Micro-Hyperspec、APEX、AisaEAGLE、Nano-Hyperspec和VNIR E-Series, 虽然这些传感器的光谱分辨率在3–7 nm, 但仍可以利用FLD或者3FLD等算法对O_2-A吸收波段进行SIF的反演, 从而获取SIF的空间分布图(Wu *et al*., 2022a)。与传统成像高光谱传感器不同, HyPlant、CFIS和FIREFLY是专门为观测SIF而设计的光谱分辨率达到亚纳米级的成像超高光谱传感器。其中, HyPlant机载成像系统作为欧洲航天局FLEX卫星任务测试的核心演示器, 由两个模块组成: 用于测量可见光和近红外光谱区域的表观反射率的宽带双通道模块(DUAL)和用于SIF反演具有超高光谱分辨率的荧光模块(FLUO)。FLUO的光谱分辨率为0.25 nm, 是首个具备全波段SIF反演的机载传感器。HyPlant也是目前最成熟的机载成像SIF系统, 已被广泛应用于生产力监测、胁迫监测和生物多样性等研究(Rossini *et al*., 2015a; Wieneke *et al*., 2016; Colombo *et al*., 2018; Gerhards *et al*., 2018; von Hebel *et al*., 2018; Tagliabue *et al*., 2020; Damm *et al*., 2022; Zeng *et al*., 2022a)。此外, 美国研制了两套机

DOI: 10.17521/cjpe.2022.0233

载成像SIF观测系统, 其中CFIS是为验证OCO-2卫星的SIF反演而开发的成像系统, 其光谱分辨率小于0.1 nm, 光谱覆盖范围为737–772 nm, 可用于远红波段SIF (FRSIF)反演(Sun *et al*., 2017; Frankenberg *et al*., 2018)。另一个由Headwall公司研发的超高光谱分辨率叶绿素荧光传感器FIREFLY, 其光谱分辨率小于0.2 nm, 光谱覆盖范围为670–780 nm, 可以实现红波段SIF (RSIF)和FRSIF反演(Paynter *et al*., 2020; Belwalkar *et al*., 2022)。与无人机非成像SIF观测相似, 机载成像SIF观测同样面临大气干扰的问题, 需要进行大气校正。此外, 机载成像SIF的数据量庞大, 飞行成本昂贵, 研发与应用仍处于早期阶段, 有待进一步探索与研究。

1.2.3 卫星观测

近年来, SIF卫星遥感反演技术得到了长足的发展, 已经成功利用多个卫星平台的高光谱数据生成了全球SIF产品。如表3所示, 可用于SIF反演的卫星传感器主要有GOSAT (Frankenberg *et al*., 2011; Joiner *et al*., 2011), SCIAMACHY (Köhler *et al*., 2015b), GOME-1 (Joiner *et al*., 2013), GOME-2 (Joiner *et al*., 2013), OCO-2 (Sun *et al*., 2018), TanSat (Du *et al*., 2018), TROPOMI (Köhler *et al*., 2018)和OCO-3 (Taylor *et al*., 2020)。Guanter等(2007)基于MERIS卫星数据, 首次在景观尺度上实现了SIF反演, 并证明了卫星数据反演SIF的可行性。Frankenberg等(2011)和Joiner等(2011)基于GOSAT卫星数据绘制了全球首张SIF地图。此后, 基于不同的卫星平台产生了多种全球卫星SIF产品。由于原始卫星SIF反演产品存在空间不连续或者时空分辨率较低等问题, 已有多个研究基于原始SIF反演产品结合MODIS反射率等辅助数据采用机器学习、深度学习等方法获取空间连续且时空分辨率改善的SIF数据集, 结合MODIS等辅助数据采用机器学习、深度学习等方法获取空间连续且时空分辨率得到改善

表3 日光诱导叶绿素荧光(SIF)的卫星数据产品
Table 3 Satellite-based data products for solar-induced chlorophyll fluorescence (SIF)

数据产品 Data product	传感器 Sensor	时间分辨率 Temporal resolution (d)	空间分辨率 Spatial resolution	时段 Time period	参考文献 Reference
GOSAT-Caltech	GOSAT	3	直径10 km Diameter 10 km	2009–2020	Frankenberg *et al*., 2011
SCIAMACHY-GFZ	SCIAMACHY	~3	1.5° × 1.5°	2002–2012	Köhler *et al*., 2015b
GOME-F	GOME-1	3	40 km × 40 km	1995–2003	Joiner *et al*., 2013
	GOME-2			2007–2019	
GOME-2-GFZ	GOME-2	1	0.5° × 0.5°	2007–2012	Köhler *et al*., 2015b
GOME-2-Caltech	GOME-2	1	0.5° × 0.5°	2007–2018	Köhler *et al*., 2015b
Downscaled-GOME2-SIF*	GOME-2	8	0.05° × 0.05°	2007–2018	Duveiller *et al*., 2020
RSIF*	GOME-2	14	0.5° × 0.5°	2007–2017	Gentine & Alemohammad, 2018
Harmonized SIF*	SCIAMACHY	~30	0.05° × 0.05°	2002-2018	Wen *et al*., 2020
	GOME-2				
DSIF*	GOME-2	16	0.05° × 0.05°	2007–2019	Ma *et al*., 2022
OCO-2_L2_Lite_SIF	OCO-2	16	2.25 km × 1.29 km	2014–2022	Sun *et al*., 2018
CSIF*	OCO-2	4	0.05° × 0.05°	2000–2020	Zhang *et al*., 2018a
SIF_{oco2_005}*	OCO-2	16	0.05° × 0.05°	2014–2021	Yu *et al*., 2019
GOSIF*	OCO-2	8	0.05° × 0.05°	2000–2020	Li & Xiao, 2019
TanSat SIF	TanSat	16	2.0 km × 2.0 km	2017–2019	Du *et al*., 2018
Continuous TanSat SIF*	TanSat	4	0.05° × 0.05°	2017–2019	Ma *et al*., 2020
IAPCAS/SIF	TanSat	16	1.0° × 1.0°	2017–2018	Yao *et al*., 2021
TROPOMI-Caltech	TROPOMI	8	0.05° × 0.05°	2018–2021	Köhler *et al*., 2018
TROPOSIF	TROPOMI	~1	3.5 km × 5.5 km	2018–2021	Guanter *et al*., 2021
SIFnet*	TROPOMI	16	0.005° × 0.005°	2018–2021	Gensheimer *et al*., 2022
OCO3_L2_Lite_SIF	OCO-3	16	2.25 km × 1.29 km	2019–2022	Taylor *et al*., 2020

部分数据产品提供多种时间分辨率和空间分辨率产品, 表格所列时间分辨率和空间分辨率均是其所提供最高的时间分辨率和空间分辨率。数据产品名称后面带*表示该产品属于重构SIF产品。
Some data products provide a variety of time resolution and spatial resolution, and the time resolution and spatial resolution listed in the table are the highest. Data product name is followed by * indicating that the product belongs to the reconstructed SIF product.

的SIF数据集。例如, Downscaled-GOME2-SIF (Duveiller *et al*., 2020), RSIF (Gentine & Alemohammad, 2018), GOSIF (Li & Xiao, 2019), CSIF (Zhang *et al*., 2018a), Harmonized SIF (Wen *et al*., 2020), DSIF (Ma *et al*., 2022), Continuous TanSat SIF (Ma *et al*., 2020)和SIFnet (Gensheimer *et al*., 2022)。然而, 这些重建SIF产品可能受到辅助数据集和机器学习方法等的不确定性影响, 并不一定能反映植物真实发射的SIF信号。

目前已有的卫星均不是专门为SIF探测而设计, 只是这些亚纳米级分辨率的波段与荧光的发射波段重叠。未来, 欧洲航天局FLEX任务的FLORIS传感器是专门为获取SIF信号设计, 其空间分辨率将达到0.3 km, 这将为更精细地监测陆地植被光合动态提供新的可能(Drusch *et al*., 2017)。然而, 由于卫星自身物理性能的限制, 空间分辨率和时间分辨率相互制约, 在SIF与GPP机理关系、卫星SIF遥感数据同化、植被物候和胁迫监测等领域仍存在较多问题, 需要进一步研究。

1.3 反演算法

在遥感传感器接收到的地表反射的光谱信号中, 叶绿素荧光部分所占比重非常小, 因此从遥感光谱数据中分离出荧光信号较为困难(Meroni *et al*., 2009)。然而, 光谱信号中具有许多太阳和地球大气吸收特征波段, 在这些吸收特征波段内, 辐射亮度信号较弱, 荧光信号在这些吸收特征波段占据的比例达到最大, 即荧光会对吸收特征波段进行一定的填充, 从而改变探测到的植被反射率。在可见光与近红外波段, 具有两个氧气吸收特征波段, 分别为O_2-B (687 nm)与O_2-A (760 nm), 以及一些太阳大气吸收特征, 这些吸收特征表现为波段宽度0.1–10 nm的暗线。荧光反演是基于荧光对于吸收波段深度的填充来分离荧光与辐亮度, 通过比较有无荧光贡献的光谱吸收波段的深度来进行荧光的提取, 这一原理称之为夫琅禾费光谱线填充原理(Fraunhofer line discrimination, FLD)。如表4所示, 根据反演SIF所用的波段, 反演算法大致可以分为两大类: 基于地球大气吸收线(主要是O_2-A和O_2-B)和基于太阳夫琅禾费光谱线(Mohammed *et al*., 2019)。根据反演的SIF波段和范围, 也可以分为单波段反演算法和全波段反演算法, 其中全波段算法是基于单波段算法反演640–850 nm范围内的多个吸收暗线波段的SIF, 结合先验函数或主成分重构全波段SIF (Zhao *et al*., 2014, 2018; Cogliati *et al*., 2015b; Liu *et al*., 2015)。

基于大气吸收波段(O_2-A和O_2-B)的SIF反演算法发展以FLD为基础, 通过对荧光与反射率的假设从最初的具体化到泛化的发展, 产生一系列改进算法, 包括3FLD (Maier *et al*., 2004; Damm *et al*., 2014), cFLD (GomezChova *et al*., 2006), iFLD (Alonso *et al*., 2008; Wieneke *et al*., 2016), pFLD (Liu & Liu, 2015)以及SFM (Meroni & Colombo, 2006; Guanter *et al*., 2010; Meroni *et al*., 2010; Mazzoni *et al*., 2012)等。以上算法适用于近地面SIF反演, 然而, 这些算法应用到高度较高的塔基或者机载无人机观测则需要进行大气吸收的校正(Porcar-Castell *et al*., 2021)。

与基于地球大气吸收波段的反演算法相比, 基于太阳吸收特征的反演算法不需要复杂的大气模型。因此, 基于太阳夫琅禾费光谱线的反演算法被广泛应用于星载SIF反演(Mohammed *et al*., 2019)。这类算法可以分为两类: 基于物理模型的反演算法和基于数据驱动统计的反演算法(纪梦豪等, 2019; 王思恒等, 2019)。基于物理模型的反演算法, 可以通过简化辐射传输方程, 使用更窄的窗口, 获取信噪比更高, 噪声更小的SIF信号(Frankenberg *et al*., 2011; Joiner *et al*., 2011, 2012; Köhler *et al*., 2015a)。差分光学吸收光谱(DOAS)算法也是常用基于物理模型的反演算法, 其利用大气散射和大气分子吸收引起光学厚度变化随波长变化的差异来识别气体成分并反演气体浓度(Platt & Stutz, 2008)。基于数据驱动统计的反演算法从光谱数据本身的特性出发, 利用数学统计方法表征光谱的结构信息。这类算法基于简化的大气辐射传输方程, 将传感器接收到的辐亮度信号表征为光谱平滑项(荧光光谱和反射率光谱)和光谱非平滑项(夫琅禾费吸收线特征)的组合, 并利用最小二乘法就可以将SIF信号提取出来(Guanter *et al*., 2012)。通过PCA或者SVD等方法将非线性的大气层顶辐射使用方程转化为用少数主成分代表的线性方程, 进而求解出SIF (Guanter *et al*., 2012, 2013; Joiner *et al*., 2013, 2016; Köhler *et al*., 2015b; Du *et al*., 2018; Yao *et al*., 2022)。基于数据驱动统计的反演算法能有效地提高SIF反演的效率, 且在一定程度降低了对光谱分辨率和大气辐射传输的要求, 但其受选取的训练数据集、反演波段

DOI: 10.17521/cjpe.2022.0233

表4 日光诱导叶绿素荧光(SIF)的主要反演算法
Table 4 Main retrieval methods of solar-induced chlorophyll fluorescence (SIF)

反演算法 Retrieval method	SIF波段/范围 SIF bands/spectral range (nm)	反演窗口内对SIF形状的假设 Assumed SIF spectral shape in the retrieval window	反演窗口内对反射率形状的假设 Assumed reflectance spectral shape in the retrieval window	适用平台 Suitable for platforms	参考文献 Reference
FLD	O_2-A, O_2-B	恒定 Constant	恒定 Constant	近地面 Near-surface	Plascyk, 1975
3FLD	O_2-A, O_2-B	线性 Linear	线性 Linear	近地面 Near-surface	Maier *et al*., 2004
cFLD	O_2-A, O_2-B	校正系数调节 Adjusted with correction factor	校正系数调节 Adjusted with correction factor	近地面 Near-surface	GomezChova *et al*., 2006
iFLD	O_2-A, O_2-B	校正系数调节 Adjusted with correction factor	校正系数调节 Adjusted with correction factor	近地面 Near-surface	Alonso *et al*., 2008
pFLD	O_2-A, O_2-B	校正系数调节 Adjusted with correction factor	校正系数调节 Adjusted with correction factor	近地面 Near-surface	Liu & Liu, 2015
SFM	O_2-A, O_2-B	多项式或其他函数 Polynomial or other function	多项式或其他函数 Polynomial or other function	近地面、卫星 Near-surface, satellite	Meroni *et al*., 2010
SVD	Far-red	恒定 Constant	奇异向量 Singular vectors	近地面、卫星 Near-surface, satellite	Guanter *et al*., 2012
PCA	Far-red	高斯函数拟合 Gaussian	多项式拟合 Polynomial	卫星 Satellite	Joiner *et al*., 2014
DOAS	Red, Far-red	参考光谱或高斯函数 Reference spectrum or Gaussian	多项式拟合 Polynomial	近地面、卫星 Near-surface, satellite	Wolanin *et al*., 2015
FSR	640–850 nm	多项式拟合 Polynomial	多项式拟合 Polynomial	近地面 Near-surface	Zhao *et al*., 2014
F-SFM	645–805 nm	线性组合 Linear combination of basis spectra	线性组合 Linear combination of basis spectra	近地面 Near-surface	Liu *et al*., 2015
SpecFit	670–780 nm	伪福格特函数 Pseudo-voigt	分段三次样条函数 Piecewise cubic spline	近地面 Near-surface	Cogliati *et al*., 2015b

O_2-A和O_2-B分别指氧气在760和687 nm附近的吸收波段。Red和Far-red分别指红波段和近红外波段, 波段范围与所选的太阳和地球大气吸收特征波段有关。
O_2-A and O_2-B refer to the absorption bands of oxygen near 760 and 687 nm, respectively. Red and Far-red refer to the red band and near-infrared band respectively, and the band range is related to the selected solar fraunhofer and telluric absorption features.

和各成分的拟合函数(包括多项式的阶数、选取主成分的个数和荧光函数的拟合)的限制, 仍有待进一步的研究。

2 SIF在陆地生态系统监测中的应用

2.1 生态系统功能

生态系统功能是指生态系统内部及其与外部环境之间的联系与相互作用, 主要表现为能量流动、物质循环和信息传递, 它决定了生态系统提供服务的质量与总量(Odum & Barrett, 1971)。新兴的SIF遥感技术为生态系统功能的研究带来了新机遇, 其与植物光合作用的密切联系, 可以为生态系统能量流动与物质循环过程中的关键要素(例如生理生化组分和生产力)反演提供新的手段(Ryu *et al*., 2019; 郭庆华等, 2020; Porcar-Castell *et al*., 2021)。

2.1.1 生理生化组分

生理生化组分是体现生态系统活力和衡量生态系统特征的重要指标, 是植物在表征生态系统功能方面的生态指示, 也是反映生产能力、环境适应性等属性的重要植物功能性状(孟婷婷等, 2007; 郭庆华等, 2020)。植被光能利用率(LUE)是生态系统或植物群落每吸收1 mol光量子而固定的大气中CO_2的物质的量, 是表征生态系统水平植物群落对光能的利用效率(Grace *et al*., 2007)。理论上, LUE与非光化学淬灭系数(NPQ)、SIF量子产率(SIF_{yield})关系密切且通常是此消彼长的关系, 因此很多研究从模型模拟、叶片尺度、冠层尺度和全球区域尺度探讨了SIF或者SIF_{yield}与LUE的关系(Freedman *et al*., 2002; Damm *et al*., 2010; Liu & Cheng, 2010; Liu *et al*., 2013a; Porcar-Castell *et al*., 2014; Yang *et al*., 2015, 2018a; Zhang *et al*., 2016, 2018b; Miao *et al*., 2018; Li *et al*., 2020c; Wu *et al*., 2022a), 结果表明, SIF_{yield}与LUE的关系受植被类型、光照条件和冠层结构等因素影响, 在低光照条件下负相关, 高光照条件下呈正相关关系(Porcar-Castell *et al*., 2014); 此外, 由于冠层尺度的光合作用影响因素复杂, 叶片尺度的SIF_{yield}与LUE关系优于冠层尺度的关系(Wu *et al*., 2022a)。

植物叶片最大羧化速率(V_{cmax})是表征植物光合能力的关键参数, 精确模拟V_{cmax}有助于准确预测植

物的光合作用和陆地生态系统生产力(张彦敏和周广胜, 2012; 闫霜等, 2014)。Zhang等(2014)首先将GOME-2卫星SIF数据与SCOPE模型相结合, 推算出V_{cmax}的季节变化模式。此后一系列研究基于实测和模型数据深入探讨了SIF-V_{cmax}的关系(Koffi *et al*., 2015; Verrelst *et al*., 2015; van der Tol *et al*., 2016; Zhang *et al*., 2018c; Camino *et al*., 2019; Fu *et al*., 2020; Li *et al*., 2020a), 大多数研究表明SIF具有估算V_{cmax}的潜力, 然而, 少数研究表明在高光照条件下SIF对V_{cmax}的敏感性很弱(Koffi *et al*., 2015)。近期, Han等(2022b)利用光反应与碳反应(暗反应)的平衡, 推导出叶绿素荧光激发与光合能力参数的理论方程, 并对光系统II (PSII)的理论叶绿素荧光激发总量(SIF_{PSII})与V_{cmax}和最大电子传递速率(J_{max})之间的动态关系提出可检验的假设。结果表明, PSII的氧化还原状态强烈影响SIF_{PSII}与V_{cmax}和J_{max}的关系, 而$SIF_{PSII} \times q_L$ (q_L表示PSII反应中心开放程度)表明了PSII的氧化还原状态, 是V_{cmax}和J_{max}的有效预测因子。

叶绿体是植物进行光合作用的场所, 叶绿素具有吸收转换光能的作用。因此, 植物叶片叶绿素含量(LCC)的变化是影响光合速率的重要因素(Gitelson *et al*., 2005; Croft *et al*., 2020)。由于LCC控制着SIF的激发量, 同时对不同波段的SIF的重吸收比例不同, 因此也是导致不同尺度和不同波段的SIF差异的重要因素(Verrelst *et al*., 2015; Liu *et al*., 2019c, 2020b; Zhang *et al*., 2021b)。大量研究表明, 在叶片尺度, RSIF与FRSIF的比值与LCC存在很好的幂函数关系(Gitelson *et al*., 1998; Tubuxin *et al*., 2015; Li *et al*., 2020a)。基于此, 利用叶片尺度的RSIF与FRSIF比值可以很好地估算LCC (Tubuxin *et al*., 2015)。

氮是合成叶绿素和与光合有关蛋白的重要成分, 植物体内75%的氮都集中于叶绿体中, 且大部分都用于光合器官的构建, 因此它是光合物质代谢和植物生长的关键因子(Evans, 1989; 郑淑霞和上官周平, 2007)。鉴于植物叶片氮含量(LNC)与叶片光合能力密切相关, 及主动荧光动力学参数可以反映植物LNC的动态变化, SIF理论上也具有探测LNC的潜力(Berger *et al*., 2020)。Jia等(2018)在叶片尺度基于SIF对LCC的响应, 评估了SIF定量估算LNC的可行性。Camino等(2018)研究发现, 与仅基于LCC、干物质或等效水厚度建立的模型相比, 引入SIF的LNC反演可以获得更高的精度。Jia等(2021)进一步在冠层尺度上基于SIF估算LNC, 并根据SIF、光合作用和LNC之间的关系, 评估了SIF指数定量估算光合作用氮利用效率的潜力。

2.1.2 植被生产力监测

总初级生产力(GPP)是初级生产者(一般是植物)通过光合作用将无机碳转化成有机物的量, 是表征生态系统物质生产和能量流动的关键因子(Field *et al*., 1995; Anav *et al*., 2015)。近十年来, SIF被广泛应用于陆地生态系统GPP估算, 其理论基础是光能利用率模型(Monteith, 1972):

$$GPP = PAR \times fPAR \times LUE \quad (1)$$

式中, PAR为到达植被冠层的光合有效辐射; fPAR为植被吸收光合有效辐射比。PAR与fPAR的乘积表示植物吸收的光合有效辐射(APAR)。类比于GPP的定义, SIF可以表示为(Guanter *et al*., 2014):

$$SIF = PAR \times fPAR \times \Phi_F \times f_{esc} \quad (2)$$

式中, Φ_F为荧光量子效率, 即吸收的PAR转化为荧光的比例; f_{esc}为叶片发射的荧光逃逸冠层的概率, 其主要受到冠层结构和叶绿素含量的影响。由公式(1)和(2)可知, SIF与GPP之间的关系主要由共同因子APAR驱动。由此, SIF与GPP之间的关系可以表示为:

$$GPP = SIF \times \frac{LUE}{\Phi_F \times f_{esc}} \quad (3)$$

公式(3)描述的SIF与GPP的关系简化了一系列复杂的机制, 是一个描述SIF与GPP之间耦合关系的简单模型。由此, 建立了基于SIF估算陆地生态系统GPP的理论基础。

大量研究表明, 冠层尺度SIF与GPP关系在不同生态系统呈显著正相关关系(Frankenberg *et al*., 2011; Sun *et al*., 2017; Zhang *et al*., 2019b, 2020b; Li & Xiao, 2022)。然而, 由于SIF与GPP关系模型受环境因子、冠层结构、植物光合作用途径及时空尺度等多种因素的影响(Magney *et al*., 2020), 不同生态系统的SIF与GPP关系存在差异(Damm *et al*., 2015)。例如, 由于植物光合途径不同, C_3和C_4植物的SIF-GPP的线性关系的斜率存在差异(Liu *et al*., 2017; Zhang *et al*., 2020b)。在全球尺度, Frankenberg等(2011)发现SIF与GPP存在很好的线性关系; 在区域尺度上, Guanter等(2014)通过星载GOME-2的SIF

DOI: 10.17521/cjpe.2022.0233

数据与美国玉米(*Zea mays*)带农田生态系统和西欧草原的涡度通量站点GPP数据建立了简单的线性回归关系; 而在站点尺度, 0.5 h时间分辨率的SIF与GPP模型则不是简单的线性关系。例如, Goulas等(2017)通过对小麦(*Triticum asetivum*)站点数据分析发现, SIF-GPP的简单线性关系可能只存在于绿色生物量变化明显且光能利用率变化较小的情景; Li等(2020c)通过对玉米站点数据分析发现, 0.5 h尺度的SIF-GPP的非线性关系优于线性关系。不同环境因子影响下的SIF-GPP的关系也存在差异。例如, Li等(2020c)发现不同天空条件(阴天和晴天)会影响SIF-GPP的关系模型; Wieneke等(2018)发现胁迫条件会解耦SIF-GPP的线性关系。总的来说, 在不同生态系统间、不同时空尺度下和不同环境因子影响下的SIF-GPP的关系仍然需要更多的研究, 以更好地服务于陆地生态系统的GPP的精确估算。

陆面模式(LSM)是地球系统模型的关键组成部分, 可在区域和全球尺度模拟陆地表面与大气界面的碳、水通量和能量交换。Lee等(2015)将SIF和光合作用的耦合模块加入NCAR CLM4 (National Center for Atmospheric Research Community Land Model version 4)模型, 使得模拟全球尺度的SIF成为可能。Koffi等(2015)将SCOPE模型耦合到BETHY (Biosphere Energy Transfer Hydrology)模型, 使得SIF在碳同化系统中的应用成为可能, 并显著减小了模型中GPP估算的不确定性。Qiu等(2019)构建了适用于不同生态系统类型的荧光多次散射模拟方法, 发展了综合考虑发射、吸收和散射过程的冠层荧光计算方案, 并将该方案耦合到BEPS模型, 揭示了冠层结构对不同尺度SIF-GPP关系的影响, 有助于降低碳循环模拟的不确定性。Wang和Frankenberg (2022)评估了在CliMA Land模型使用5种不同的冠层复杂程度时冠层碳、水和SIF通量的差异, 表明在模型中添加复杂冠层的必要性。然而, 在陆面模式中耦合SIF仍需更多探索, 以更好地估算陆地生态系统生产力和精确地模拟全球尺度碳、水和能量循环。

2.2 生态系统过程

生态系统过程是生态系统中生物和非生物通过物质和能量驱动的复杂相互作用的结果(李奇等, 2019)。陆地生态系统包含一系列时空连续、尺度多元且互相联系的生态学过程(Chambers *et al*., 2007; 岳跃民等, 2008)。近年来, 人类活动和气候变化对生态系统结构和功能产生了大规模的影响, 因此, 监测陆地生态系统的关键过程如何响应与适应全球气候变暖是全球变化生态学的基本科学问题之一(夏建阳等, 2020; 于贵瑞等, 2021)。SIF遥感能够直接表征植物生理生态过程, 被广泛应用于监测植被对极端气候的响应与适应(Song *et al*., 2018)、植被光合物候的动态特征(Wang *et al*., 2019b)及蒸腾作用的变化(Shan *et al*., 2019)等。

2.2.1 胁迫

在植物非生物胁迫的早期探测上, 理论上SIF比传统的遥感植被指数更具有优势。其理论基础是植物在遭受非生物胁迫(干旱、热害、除草剂、氮等)的早期, 其表观的绿度(叶绿素含量)和结构(叶面积指数)不会立即发生变化, 但其生理过程(如光合作用)则会立即发生响应以应对胁迫造成的损害。SIF作为光合作用的探针, 被认为是植被非生物胁迫早期探测的有效工具。

近年来, 极端天气频发, 全球绝大部分地区农业和生态干旱事件的发生频率和强度都在增加, 及时精确地监测大范围干旱胁迫对确保粮食安全和了解植被对气候变化的响应具有重要意义(Breshears *et al*., 2005)。由于干旱胁迫会引起植物一系列的生理反应, 例如叶片气孔关闭导致光合速率下降, NPQ上升, 因此SIF可以直接反映出植被对干旱胁迫的快速响应(Perez-Priego *et al*., 2005)。绝大多数地面实验研究表明, 在干旱胁迫的影响下, 植物冠层SIF会下降(Daumard *et al*., 2010; Wieneke *et al*., 2018; Xu *et al*., 2018, 2021; Liu *et al*., 2020a; Chen *et al*., 2021)。Xu等(2018)以玉米为对象, 通过近地面遥感平台获取高时间分辨率的SIF数据, 研究发现, 在干旱胁迫下, 由于冠层结构和光合作用共同调节, RSIF和FRSIF都会发生下降。此外, 复水后, FRSIF会明显升高, RSIF也有一定升高, 但升高幅度没FRSIF明显。Chen等(2021)使用连续3年的塔基观测数据, 研究了玉米在日变化和季节变化的尺度上SIF和GPP之间的关系及其对干旱胁迫的响应, 研究发现, 随着干旱胁迫程度的增加, GPP与SIF的比值下降, 冠层气孔导度同步下降, 证明了SIF数据不仅包含冠层结构信息也包含了大量的生理信息, 可以作为监测干旱和估算GPP的潜在指标。

同样, 基于卫星SIF的全球和区域尺度的结果

也表明, 干旱胁迫下, 植物的SIF值会明显下降(Lee *et al*., 2013; Sun *et al*., 2015; Zhang *et al*., 2019a, 2020a; Li *et al*., 2020b; Liu *et al*., 2021; Qiu *et al*., 2022)。Lee等(2013)对亚马孙热带雨林的水分胁迫进行了分析, 结果表明在2010年极度干旱的条件下, 亚马孙热带雨林对大气碳吸收量减少, 传统植被指数仅能捕捉到由于叶片损失或者叶绿素含量变化导致的反射率的变化, 而SIF可以直接反映出植被由于水分胁迫, 导致气孔关闭, 造成GPP减少这一事实。因此SIF为大尺度GPP动态变化监测提供了有效工具。2011年美国得克萨斯州和2012年中部大平原发生了两种不同类型的干旱, Sun等(2015)采用GOME-2 SIF分析了两次干旱事件对作物的影响。结果表明, 在空间分布上, SIF距平的空间分布图与美国干旱程度空间分布图有很好的相关关系, 在年内季节变化上, 也可以很好地反映出干旱对作物光合作用的影响, 该研究很好地证明了SIF可以作为农作物光合作用的直接表征, 能够估算农作物的结构特征及生理状态变化。总的来说, SIF响应干旱胁迫机制主要归因于植物应对水分亏缺时, 关闭气孔并产生一系列的光保护机制, 最终导致NPQ升高和SIF降低(Jonard *et al*., 2020)。然而, 有些研究表明干旱胁迫或者人为诱导气孔关闭时, 相对于净光合速率和气孔导度, SIF并没有显著下降(Helm *et al*., 2020; Marrs *et al*., 2020)。这可能由于冠层观测SIF除了包含生理信号, 还耦合冠层结构、光照条件等非生理信号, 会干扰其表征植物响应胁迫的真实生理动态变化。

高温对植物的影响主要表现在以下3个方面: 第一, 高温增强了植物的蒸腾作用, 使其失水过多; 第二, 高温会影响植物体内的各种生理生化反应所需的酶的活性, 从而影响其生长代谢; 第三, 当高温发生时, 植物为了减少蒸腾, 气孔导度下降甚至气孔完全关闭, 进入植物体内的CO_2减少, 抑制光合作用, 有机物的积累随之减少(Berry & Bjorkman, 1980)。高温和随之而来的高水汽压亏缺(VPD)往往会对植物造成胁迫, 因此, 高温胁迫往往伴随着干旱胁迫, 但不会立即引起植物冠层结构和相应光谱特征的显著变化(Dobrowski *et al*., 2005; 章钊颖等, 2019)。诸多研究表明, 植物的SIF值在高温和干旱胁迫条件下都会下降(Ač *et al*., 2015; Rossini *et al*., 2015b; Song *et al*., 2018, 2020; Wieneke *et al*., 2018; Wang *et al*., 2019c; Qiu *et al*., 2020)。在地面增温实验中, Kimm等(2021)发现受与高温胁迫相关的冠层结构和植物生理变化的影响, SIF_{yield}会显著下降, 进一步消除冠层结构影响后的Φ_F在响应生理胁迫方面胜过包含结构信息的SIF_{yield}。Song等(2018)利用卫星SIF数据对印度恒河平原2010年小麦高温胁迫进行了综合的研究, 研究发现相比传统植被指数, SIF由于包含了小麦生理信息和冠层结构信息, 使得SIF对此次高温胁迫监测具有更快的响应时间以及更高的灵敏性。因此, 究竟是冠层SIF的生理信息, 还是非生理信息, 还是耦合着生理与非生理信息的冠层SIF本身, 更适合胁迫监测还有待进一步研究。

此外, SIF遥感也被应用于其他胁迫研究。除草剂胁迫通过阻断氨基酸、类胡萝卜素及脂类生物合成, 或者干扰细胞分裂、阻断光合作用光系统的电子传递等方式对植物造成胁迫甚至杀死植物(Culpepper & York, 1999; Taiz *et al*., 2015)。这种快速特殊的胁迫方式被广泛应用于光合作用和调制荧光的研究(Schreiber *et al*., 1986; Lichtenthaler & Rinderle, 1988; Wang *et al*., 2018), 同样也被应用于SIF与光合作用的机理研究和SIF传感器的测试(Liu *et al*., 2013b; Rossini *et al*., 2015a; Pinto *et al*., 2016, 2020; van der Tol *et al*., 2016; Celesti *et al*., 2018; Wu *et al*., 2022b)。Rossini等(2015a)在草皮上喷洒除草剂, 测试新研制的机载SIF传感器(HyPlant)观测草皮冠层SIF的动态, 研究发现, RSIF和FRSIF均能迅速捕获到草皮对除草剂的响应, 两者都先迅速上升, 在几天后下降, 这些现象也在小麦和玉米地被发现(Pinto *et al*., 2016)。氮是植物生长所需量最大的营养元素, 合理的氮肥使用对于农作物生长和提高作物产量至关重要。氮亏缺胁迫引起光合作用和荧光的变化更为复杂(Ač *et al*., 2015), 一方面, 由于氮胁迫会导致叶片叶绿素含量降低, 从而减少了荧光信号激发量; 另一方面, 叶绿素含量在氮亏缺状态下较低, 会导致RSIF再吸收减弱, 进而增加RSIF的发射(Ač *et al*., 2015)。通过对比不同氮处理条件下的月桂(*Laurus nobilis*)树的RSIF和FRSIF的比值(RSIF/FRSIF), 发现氮亏缺胁迫的月桂树的RSIF/FRSIF更高。Jia等(2021)通过田间实验测量不同氮处理的冬小麦叶片和冠层尺度的SIF, 发现SIF比率指数(SIF_R)和归一化SIF指数(SIF_N)具有监测叶片氮含量及反演光合作用氮利用率的潜力, 可以应

DOI: 10.17521/cjpe.2022.0233

用于作物氮胁迫监测研究(Jia *et al*., 2018, 2021)。此外, SIF也被应用于低温(Moya *et al*., 2019)和小麦条锈病(竞霞等, 2019)等胁迫监测中。

2.2.2 物候

植被物候是自然界植物受遗传因素与周围环境共同影响而产生周期性变化的生物学现象, 是表征生态系统动态及其对环境变化响应方式的重要生态系统参数, 也是气候变化最敏感的生物学指标之一(葛全胜等, 2010; 王敏钰等, 2022)。相较于传统光学遥感植被指数方法, 基于SIF的物候指标更能代表植物光合信息变化, 特别是对于北方常绿林、高生产力的热带雨林、植被稀疏的旱地生态系统和地物复杂的城市生态系统(Smith *et al*., 2018; Doughty *et al*., 2019; Magney *et al*., 2019; Zhou, 2022)。

在物候周期显著的中高纬地区的落叶阔叶林、混交林、草地和农作物的物候指标提取方面, Joiner等(2014)基于GOME-2卫星SIF数据和塔基通量GPP数据, 系统评估了多种植被类型SIF追踪GPP的季节变化能力, 结果表明SIF提取的植物物候周期短于基于MODIS fPAR产品的提取结果, 且与塔基通量GPP提取结果更为接近。Yang等(2015)使用地基SIF自动观测系统对落叶林进行长时序连续观测, 表明地基SIF具备观测植物物候的潜力。Walther等(2016)基于卫星数据对北美中高纬度落叶林进行物候研究, 研究结果表明基于植被指数的物候生长季结束日期晚于SIF, 这与对我国长白山温带红松(*Pinus koraiensis*)阔叶林的研究结果(刘啸添等, 2018)一致。这是由于落叶林进入秋季衰老期后, 植被光合作用虽然大幅度减弱并趋于停止, 但叶片绿度并不会迅速反映这种改变, 而是存在一个渐变过程, 因此基于SIF提取的物候生长季长度短于基于归一化植被指数(NDVI)的结果(Jeong *et al*., 2017)。农作物的物候期显著(Li *et al*., 2020a, 2020c; Zhao *et al*., 2022a), 然而不同波段SIF反映的物候动态不同。Daumard等(2012)的研究表明, 在高粱(*Sorghum bicolor*)生长初期, RSIF迅速上升, 随后趋于饱和, 而FRSIF则继续增加。这可能是由于叶绿素对RSIF重吸收所致, 因此在冠层尺度及全球尺度, FRSIF更适合作为光合物候监测指标(Meroni *et al*., 2011; Middleton *et al*., 2018)。

在北方常绿针叶林生态系统, 光合作用会发生季节性变化, 而冠层结构或者叶绿素含量没有显著变化, 基于NDVI等植被指数难以捕获常绿针叶林的物候动态。此时, 可以表征光合作用的SIF在监测其物候动态时具有独特优势(Walther *et al*., 2016)。基于GOME-2卫星SIF数据的北方常绿针叶林的物候研究表明, SIF揭示的生长季开始日期要比增强植被指数(EVI)的结果提前1个月, 主要是因为北方常绿森林在春季复苏阶段受积雪影响且植被绿度变化不明显, 因此植被光合作用不能被传统的绿度指标及时地监测出来(Walther *et al*., 2016)。基于地基冠层SIF观测芬兰南部的欧洲赤松(*Pinus sylvestris*)(Nichol *et al*., 2019), 美国科罗拉多州高山生态研究站Niwot Ridge的亚高山针叶林(Magney *et al*., 2019)和加拿大萨斯喀彻温省的云杉(*Picea asperata*)(Pierrat *et al*., 2022)的季节动态表明, SIF可以有效追踪到针叶林冬季光合速率的下降, 且与GPP的季节动态高度一致。然而, Yang等(2022)进一步分析Niwot Ridge站点数据, 发现亚高山针叶林的GPP和RSIF对光照和季节环境条件响应不一致, 这说明在针叶林中使用RSIF作为物候指标具有局限性。

在热带和亚热带常绿森林, 由于常绿冠层郁闭度和覆盖度高, NDVI监测其物候存在易饱和及敏感性低的问题, SIF可以提供不同于植被绿度信息的生理功能新视角, 在常绿林物候监测中具有较大优势(周蕾等, 2020)。相比于叶绿素变化, 表征光合效率变化的SIF与亚马孙热带森林的水分胁迫表现出更高的相关性(Lee *et al*., 2013)。因此, 卫星SIF被应用于揭示亚马孙热带雨林在旱季是否正在变绿这个争议话题(Doughty *et al*., 2019; Xie *et al*., 2022)。Bertani等(2017)基于9年GOME-2卫星SIF数据评估亚马孙雨林光合活性对太阳辐射和降水的季节响应, 结果表明, 亚马孙雨林的光合季节变化79%是由太阳辐射的季节变化驱动, 13%受降水量的限制。Doughty等(2019)基于最新的TROPOMI卫星SIF数据研究表明, 亚马孙雨林SIF在旱季早期没有下降, 在旱季的后期和湿季早期有大幅度上升, 有力地证明了亚马孙在旱季变绿, 即绿度、SIF和光合都在增加。Xie等(2022)基于多种卫星数据集, 包括叶面积指数(LAI)、卫星荧光重构产品CSIF、EVI和植被光学厚度(VOD), 全面评估了亚马孙热带雨林的季节变化, 4个卫星植被数据集都显示亚马孙大部分区域植被覆盖度都表现出增长的趋势; 但植被的变化不

仅在空间上有差异, 而且不同数据集之间也有差异。部分原因可能是不同植被数据集捕捉了不同的植被物理特性。例如, LAI首先出现季节最大值, 随后CSIF、EVI和VOD依次出现最大值。Wu等(2021)基于卫星SIF数据和地面凋落物数据探究水和光的可利用性如何控制热带常绿森林的叶片物候, 发现泛亚洲热带常绿森林叶片凋落取决于降雨和入射太阳辐射季节性变化的同步性。

在干旱-半干旱生态系统, 由于植被覆盖度低, 基于植被指数的物候监测方法易受到土壤背景影响, 进而在物候参数提取结果中引入一些不确定性。然而, SIF信号几乎不受土壤背景影响。因此, 基于卫星的SIF具有改善遥感监测旱地生态系统的季节和年际GPP动态的能力(Smith *et al*., 2018, 2019)。Wang等(2019a)在澳大利亚北部地区评估了卫星SIF捕获旱地生态系统物候动态变化的能力, 发现相对于EVI, SIF提取的物候期参数不受土壤背景影响, 更为准确地表征了植被物候沿降水梯度的时空变化趋势。Dannenberg等(2020)的研究也发现, 在地上生物量较低的旱地生态系统, SIF捕获年内植被生长季动态的能力比NDVI强。此外, Wang等(2022)全面评估了基于卫星观测的长时间序列植被表征参数, 包括NDVI、NIRv等植被指数和TROPOMI卫星SIF, 捕获旱地GPP季节性变化的能力。其研究表明NIRv和SIF是最佳的GPP表征参数。两个参数在获取不同旱地生态系统类型的GPP季节性变化时具有互补作用, NIRv在生产力较低的、稀疏分布的非常绿植被站点中的表现优于其他参数, 而SIF在生产力较高的常绿植被站点中的表现优于其他参数。未来需要进一步探索融合NIRv和SIF的互补作用, 来提升我们在基于卫星的模型中对旱地生态系统GPP变化的理解和描述。

在地物复杂的城市生态系统, 城市化会导致温度和CO_2浓度的上升, 从而对植物物候产生广泛影响, 包括春季物候提前和秋季物候延迟(Zhou, 2022)。基于传统的植被指数来研究城市地区植被物候, 会面临着较为严重的混合像元问题, 非植被亚像元会对植被物候的提取造成显著的影响(Wang *et al*., 2019b)。由于SIF仅在植被进行光合作用时被激发, 非植被像元不会对SIF遥感信号产生影响。因此采用高空间分辨率SIF数据, 可以较为精确地提取城市植被的光合物候信息。Wang等(2019b)基于OCO-2卫星提供的千米级别SIF遥感数据, 提取了城市地区植被的光合物候信息, 并提出一种基于城市-郊区梯度的植被物候研究方法, 将城市地区作为温度和CO_2浓度提升情境下的控制实验组, 将郊区作为对照实验组, 研究植被在未来气候变化情景下的物候变化, 研究揭示了全球变化尤其是升温和CO_2浓度升高对植被光合作用的促进作用, 也表明城市生态系统可以作为未来自然生态系统气候变化研究的天然实验室。

2.2.3 植被蒸腾

蒸散发(ET)在地表能量交换和水分平衡中扮演重要角色, 包括地表蒸发作用(E)和植物蒸腾作用(T), 是陆地生态系统水文循环的重要过程(Chapin *et al*., 2002; Stoy *et al*., 2019)。准确监测和估算植物蒸腾的时空变化对于理解地表与大气之间的能量与水分交换过程及对全球变化的响应, 环境变量模拟与预测以及水资源调控机制的研究具有重要意义(Fisher *et al*., 2017)。一些基于卫星SIF的研究表明, 在严重干旱事件期间, 由于缺水导致气孔关闭, 从而引起光合作用、SIF和蒸腾作用下降(Lee *et al*., 2013; Sun *et al*., 2015; Yoshida *et al*., 2015)。Damm等(2018)使用SCOPE模型模拟, 提供了基于SIF估算植物蒸腾作用的见解, 然而, SIF与蒸腾作用的机理联系仍需利用地面实测数据进行研究。Lu等(2018)基于哈佛森林的站点数据探索SIF与植物蒸腾的关系, 研究发现FRSIF比RSIF对蒸腾作用变化更敏感, 尽管胁迫等因素会使得SIF与蒸腾的相关性变差, 但不同波段SIF组合可以获得蒸腾作用的准确估计。

在植被覆盖度较高的地区, 冠层参数对蒸散的模拟结果具有较大影响, 其中冠层气孔导度是植被蒸腾准确估算的关键参数(Schlesinger & Jasechko, 2014)。冠层气孔导度通常采用经验或半经验半理论参数化方法, 但因气孔导度经验模型中缺少理论基础及环境因子对气孔导度的累积效应, 光合作用模拟过程的酶动力学模型和光能利用率模型均无法准确估算不同生态系统的光合能力, 限制了模型在不同环境条件下的预测能力(Berry *et al*., 2010)。针对这一问题, Shan等(2019)利用地基观测的冠层SIF对不同生态系统冠层气孔导度和蒸腾进行模拟。相比传统的植被指数, SIF的日变化和季节变化与冠层气孔导度的变化有更高的一致性, 且相关性随着时间尺度的增大而增强。进而利用SIF估算的气孔导度对

DOI: 10.17521/cjpe.2022.0233

冠层蒸腾进行模拟, 结果表明SIF能够模拟植被蒸腾的日变化和季节变化, 但其模拟能力受植被覆盖度和土壤水的影响。Shan等(2021)进一步提出了一种半机理模型, 通过推导SIF和气孔导度以及VPD之间的解析解, 结合光合途径和最佳气孔扩散理论, 来估算植物蒸腾作用, 并在森林和农田生态系统中, 通过每小时冠层SIF和协同的涡度协方差通量观测, 验证了该模型。为了确定影响SIF对生态系统蒸腾估算能力的相关生物和非生物环境驱动因素, Damm等(2021)利用温带混交林在展叶期的观测数据和基于Penman-Monteith (PM)的模型框架, 分析了SIF对蒸腾的日动态和季节动态的敏感性, 并使用SCOPE模型来研究SIF和蒸腾对非生物和生物环境驱动因素的依赖性, 包括净辐射、空气温度、相对湿度、风速和LAI。

基于GOME-2卫星SIF数据, Alemohammad等(2017)利用人工神经网络估算了包括潜热通量在内的地表湍流通量, 并表明SIF与蒸腾具有很好的关系。Rigden等(2018)使用美国1 614个气象站数据评估了区分植物蒸腾与地表蒸发的方法, 并发现GOME-2 SIF与蒸腾具有很高的相关性, 同样, Pagán等(2019)发现PAR归一化的GOME-2 SIF与蒸腾速率(即蒸腾与潜在蒸发比值)之间存在较强的相关性。然而, 蒸腾作用的全球时空动态具有高度不确定性。Maes等(2020)基于GOME-2及OCO-2 SIF对从全球分布的通量站点推导出来的蒸腾进行比较, 发现卫星SIF与蒸腾高度相关, 表明可以在全球尺度利用卫星SIF进行可靠的植物蒸腾估算。基于此, 卫星SIF也被认为具有估算ET的巨大潜力。

以上研究揭示了SIF从站点到区域和全球尺度模拟植被蒸腾方面的潜力和优势。SIF遥感技术为研究碳水耦合过程参数的反演提供了新的思路, 对降低生态系统碳水通量模拟的不确定性, 准确预测生态系统对全球变化响应具有重要的意义。

3 讨论和展望

SIF遥感技术突破了传统主动荧光测量的尺度瓶颈及传统光学反射率遥感的生理限制瓶颈, 从叶片、冠层、景观到全球尺度提供了研究陆地生态系统光合作用的新途径(Porcar-Castell *et al*., 2021)。目前, 从地基、无人机、机载到卫星获取SIF数据, 极大地强化了连续时空的陆地生态系统监测能力。然而, 为了更好地发挥多尺度SIF观测的潜力, 仍有很多挑战需要去克服。例如, 天空地一体化观测, 数据预处理后获取可靠的SIF数据产品, 准确提取隐含在SIF信号中的植物生理信息, 对SIF机理和时空动态的深入和全面认识。在此基础上, 探索基于SIF的新兴的生态学应用, 从而更好地服务于陆地生态系统监测(图3)。

3.1 天空地一体化观测

随着SIF遥感观测平台的增加、传感器的多样化、地面观测网络的发展, 用于监测陆地生态系统的SIF时空数据越来越丰富。在时间尺度上, 地基SIF观测可以达到亚分钟尺度; 在空间尺度上, 无人机高光谱成像可以提供厘米(cm)尺度的SIF反演数据; 在空间范围上, 卫星可以提供全球尺度的SIF产品。因此, 跨平台进行天空地一体化SIF协同观测全球不同生态系统的植被光合作用尤为重要。

建立标准化的地面观测网络: 一方面可以定点、长时序、高频地获取各个生态系统的光谱和SIF数据, 协同涡度相关通量观测, 开展基于碳通量观测及地基/星载SIF与植被GPP之间耦合机制与模型研究。另一方面, 也可以为星载或机载数据提供校准和验证数据。目前, 全球主要有SpecNet、BioSpec、EuroSpec和ChinaSpec 4个光谱观测网络。其中ChinaSpec, 全称中国生态系统光谱观测研究网络, 是我国首个光谱观测网络, 于2017年开始建设, 截至2022年5月共建立了22个观测站点, 覆盖了农田、草地、森林、湿地、稀树草原、高寒草甸等生态系统(Li *et al*., 2020c; Liu *et al*., 2020b, 2022; Zhang *et al*., 2021a; Zhu *et al*., 2021; Huang *et al*., 2022; Shi *et al*., 2022)。ChinaSpec通过构建我国典型植被生态系统SIF和物候的自动监测平台, 将涡度相关通量塔、卫星、近地面植被遥感和模型综合集成起来, 有助于深入认识生态系统光合作用和植被物候对气候变化的响应和适应, 为国产碳卫星的应用提前开展相关技术研发, 也为我国主要植被生态系统碳循环机理研究、温室气体有效减排和国家宏观决策提供科技支撑。目前, 地面观测网络和近地面植被冠层SIF观测发展迅速, 然而, 不同SIF观测系统间的仪器配置、采集流程、观测方法和反演算法往往存在差异。因此需要进行标准化测量、统一校准协议、光谱质量控制、评估并考虑这些因素所造成的不确定性(Chang *et al*., 2021; 李朝晖等, 2021;

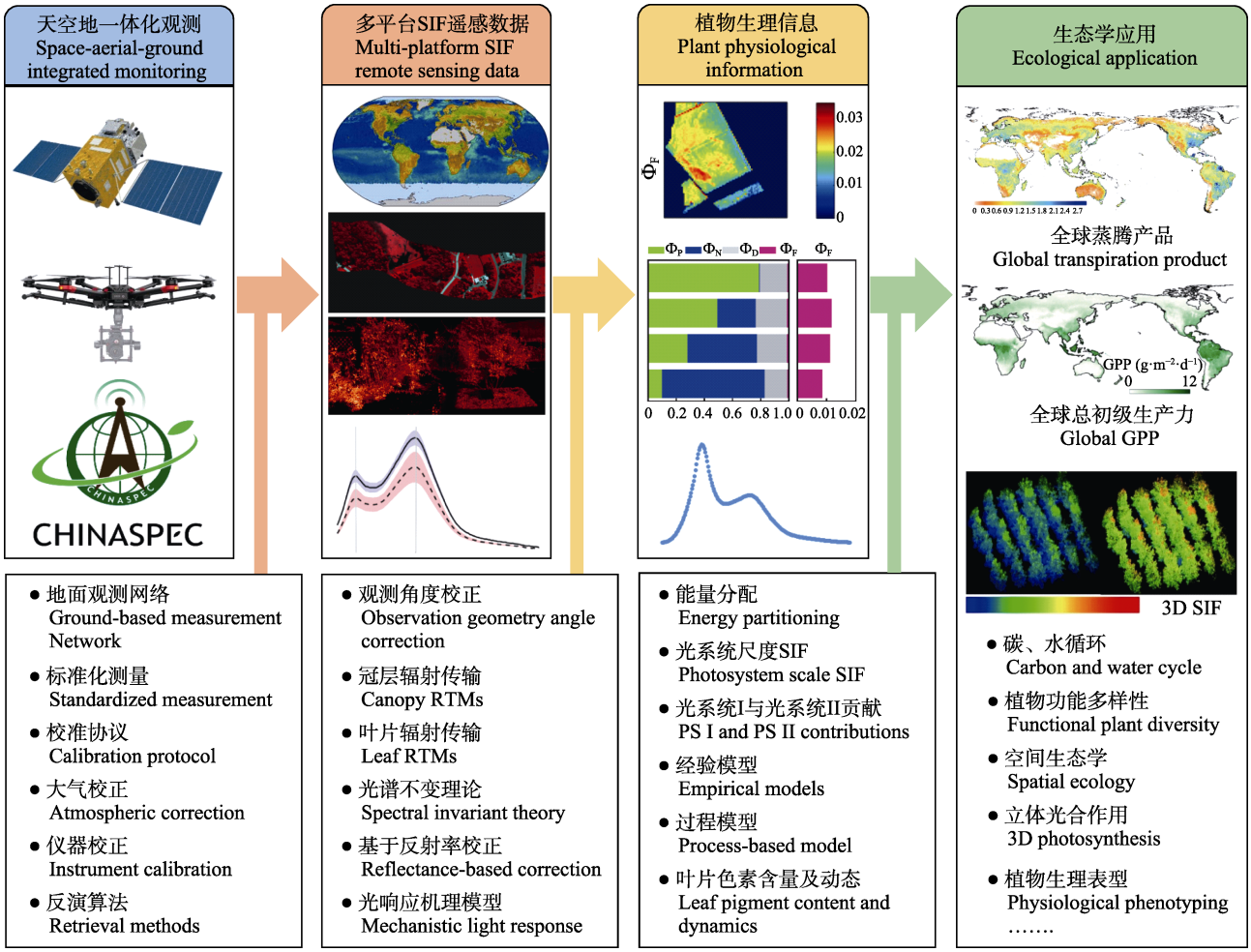

图3 日光诱导叶绿素荧光(SIF)遥感标准化数据处理与建模流程及其在生态学中的新兴与潜在应用。部分子图来源Zeng等(2022a)。Φ_D, 固有热耗散量子效率; Φ_F, 荧光量子效率; Φ_N, 非光化学淬灭量子效率; Φ_P, 光化学淬灭量子效率。

Fig. 3 A roadmap of the standardized processing and modeling of solar-induced chlorophyll fluorescence (SIF) and its emerging and potential applications in ecology. Some subplots are from Zeng *et al.* (2022a). Φ_D, constitutive heat dissipation quantum efficiency; Φ_F, fluorescence quantum efficiency; Φ_N, non-photochemical quantum efficiency; Φ_P, photochemical quantum efficiency; GPP, gross primary production; RTMs, radiative transfer models; PS, photosystem.

Buman *et al.*, 2022)。

推动机载和无人机SIF观测: 二者具有较多的优势。一是可以灵活调整高度和观测位置, 能够有效弥补地基观测的空间位置固定问题, 也能够弥合地面和卫星观测之间在尺度上的差距; 二是可以兼具高空间、高时间和高光谱分辨率, 有助于植物表型分析, 精准农业应用, 生物多样性调查, 空间异质性评估, 卫星研发的预演等(Mohammed *et al.*, 2019; Zhang *et al.*, 2022a)。然而, 目前机载和无人机SIF观测仍处于早期发展阶段, 一些技术难点需要去攻克。例如, 大气校正、系统载荷和集成、空间定位、飞行成本等。期待基于无人机的SIF系统更加方便、快捷、易用, 并研发出更轻便且高质量的超高光谱成像传感器。

卫星SIF技术的发展, 为在区域和全球尺度上监测植物光合作用提供了可靠的数据。然而, 卫星SIF遥感数据的空间分辨率低限制了其在精细尺度的应用。尽管结合MODIS等辅助数据采用机器学习、深度学习等方法获取空间连续且时空分辨率得到重构的SIF数据集, 但是这些重构SIF产品可能受到辅助数据集和机器学习方法等的不确定性影响, 并不一定能真正反映植物真实发射的SIF信号。未来, 专为SIF设计的卫星传感器FLEX的空间分辨率可达到300 m, 中国第二代碳卫星(TanSat-2)的空间分辨率也有望达到500 m, 将提供前所未有的空间分辨率的原始SIF数据(Coppo *et al.*, 2017; 刘良云等, 2022)。此外, 因为SIF捕获植物受环境或者生物因素的影响往往是高度动态的, 而目前极轨对地观测

DOI: 10.17521/cjpe.2022.0233

的卫星SIF数据的时间分辨率低, 暂时不能提供类似地基观测的日变化数据(Xiao *et al*., 2021)。2019年5月搭载于国际空间站的OCO-3是目前在轨的可以提供SIF日变化的卫星传感器, 为大尺度监测生态系统的气孔导度、光合作用和蒸腾作用的日变化特征提供新的契机(Taylor *et al*., 2020; Xiao *et al*., 2021)。尽管OCO-3具备日变化的监测能力, 但它并不是对一个定点位置进行全天连续的观测。未来, 搭载在地球静止卫星上的地球静止碳循环观测站(GeoCarb)将在85° W的地球静止轨道上运行, 并将以5–10 km的空间分辨率在北美和南美上空观测SIF (Moore *et al*., 2018)。GeoCarb使用与OCO-2类似的O_2和CO_2通道, 基于OCO-2算法进行SIF反演。在使用密集扫描模式时GeoCarb的灵活扫描策略可以每天多次测量目标区域的SIF。地球静止卫星能够提供SIF的高频观测, 使得无云污染的SIF观测越来越多。但是不同传感器观测的SIF位于不同波段, 且有不同的数据质量。另外地球静止卫星有很大幅度的观测天顶角, 观测角度对SIF的影响不容忽视(Zhang *et al*., 2018d; Xiao *et al*., 2021)。

3.2 基于SIF的植物生理信息提取

植物生理学是植物学的一个分支学科, 研究植物的所有内部活动与植物中发生的生命相关的化学和物理过程, 包括植物光合作用、植物呼吸作用和植物水分生理等(Taiz *et al*., 2015)。植物生理信息, 例如PSII量子效率(Φ_{PSII})和Φ_F等, 可以直接反映植物的物质代谢、能量转化和生长发育等的规律与机理。冠层SIF是一个特殊的光学遥感信号, 它既包含着植物的生理信息也包含着植物的结构信息(Guanter *et al*., 2014)。近年来, SIF的机理研究的一个热点方向是通过拆分冠层SIF的生理与非生理信息, 以提取准确的植物生理信息, 进而可以避免不恰当使用冠层SIF而对潜在生态过程产生偏颇的理解。

如公式(2)所示, 冠层SIF可以拆分为生理信息(Φ_F)和非生理信息(PAR、fPAR和f_{esc})。如何定量描述f_{esc}对于SIF的生理信息与非生理信息的拆分至关重要。目前, FRSIF的逃逸概率的定量研究相对成熟。Yang和van der Tol (2018)通过研究入射光和发射的FRSIF的辐射传输过程, 推导出FRSIF的冠层散射(即FRSIF的逃逸概率)与冠层顶部反射率之间的关系。Zeng等(2019)基于光谱不变理论, 提出了基于反射率的FRSIF逃逸概率估算的简单方法。基于此, 地基和卫星SIF观测方向性及角度校正取得系列进展, 从而最小化SIF的方向性导致的影响, 进而提高了估算GPP的能力(Zhang *et al*., 2020c; Hao *et al*., 2021a, 2021b, 2022)。此外, Yang等(2020)提出了一个可以用于区分FRSIF的生理与非生理信息的反射率指数FCVI, 即近红外反射率与可见光反射率之间的差。Yang等(2021)基于FCVI获取生理信息探究SIF-GPP关系的物理和生理基础, 评估冠层尺度下, PAR、fPAR和APAR对SIF-GPP的贡献, 同时使用主动荧光观测研究叶片尺度的能量分配, 以揭示光化学水平下荧光和光合作用之间的关系。Zeng等(2022a)提出了结合FRSIF和植被近红外辐亮度(NIRvR)来提取Φ_F的简单方法, 并将该方法应用于3个案例研究。其中光适应案例表明, Φ_F可以很好地展示考茨基效应; 热胁迫实验案例表明, 欧洲油菜(*Brassica napus*)、大麦(*Hordeum vulgare*)和小麦的Φ_F发生下降, 而处于生长期的玉米的Φ_F则小幅上升; 对于水分胁迫案例, 甜菜(*Beta vulgaris*)的Φ_F先升高, 下午略有下降。Wu等(2022b)基于NIRv × PAR (NIRvP)提取玉米和杂草的冠层Φ_F, 发现Φ_F先激增后缓慢下降, 且主导着FRSIF对除草剂的响应。Φ_F在不同胁迫条件下的变化仍有待更多的研究。

除了以上两种基于植被反射率指数的方法, FRSIF的生理与非生理信息的拆分方法, 还可以通过结合SCOPE模型(van der Tol *et al*., 2009)模拟进行拆分。Liu等(2019c)通过随机森林训练SCOPE模拟数据集, 将冠层尺度的FRSIF降尺度到光系统尺度的$FRSIF_{ps}$, 表明随机森林方法对于估计SIF逃逸概率是有效的。Biriukova等(2021)通过结合SCOPE模型和奇异光谱分析(SSA)的方法, 解耦了冠层FRSIF的快速变化组分(生理信息)和缓慢变化组分(非生理信息), 表明基于SSA的方法是一种很有前景的方法, 可以从地基SIF传感器获取的数据中提取SIF的生理信息。

然而, 以上的大部分方法并不适用于RSIF的生理与非生理信息的推导, 主要是因为RSIF从光系统尺度激发后到逃逸出冠层前, 除了经历散射还会被叶绿素重吸收, 辐射传输过程比FRSIF更复杂。目前RSIF的生理与非生理信息拆分的进展较少。Liu等(2019c)通过随机森林训练SCOPE模拟数据集, 将冠层尺度的RSIF降尺度到光系统尺度的RSIF, 该方法可以避免光谱不变理论在RSIF的限制。然而, 该方

法高度依赖于一维模型SCOPE的模拟数据, 对于冠层结构复杂的森林或许效果不好。此外, Liu等(2020b)基于光谱不变理论, 利用简单近似的方法, 提出基于反射率指数(Redv)将冠层尺度的RSIF降尺度到光系统尺度的RSIF, 该方法可以有效改善基于RSIF的GPP估算, 然而, 光谱不变理论不适用RSIF, 因为其缺乏物理机理的解释, 仅仅是经验性方法。因此, RSIF的生理信息提取依然是有待解决的难题。

光系统反应中心包括光系统I (PSI)和PSII, 两个光系统反应中心都可以激发荧光, 但PSII的荧光通常在总激发SIF中占主导地位, 尤其是在红波段范围, 在响应光化学和非光化学过程时, RSIF的量子产量表现出较大的变化, 包含更多植物光合作用信息(Porcar-Castell *et al*., 2014, 2021)。然而, PSI和PSII的能量分配很少被测量, 通常假设为对半分配。目前研究表明, PSI对荧光贡献相对稳定(Peterson *et al*., 2014)。因此, 定量PSII的SIF, 特别是PSII的RSIF更具科学价值。利用Φ_F来估算Φ_{PSII}在PAM测量可以实现。然而, 通过SIF测量得到Φ_{PSII}还处于研究阶段。最近, Han等(2022a)通过光响应机理模型(MLR)结合理论模型利用荧光产率推算出PSII的SIF, 并证明了在不同环境条件和不同植物功能类型下, MLR-SIF均能够准确表征光合作用, 且相比传统的FvCB模型, MLR-SIF模型通过充分利用观测SIF所携带的生理信息, 可降低估算的光合作用对参数不确定性的敏感性, 进一步证实了MLR-SIF模型的可靠性。未来研究可以利用多尺度观测冠层SIF推算出PSII的SIF, 从而更准确地提取植物生理信息。

3.3 SIF遥感的生态学应用展望

SIF遥感已经提供了全球尺度监测陆地生态系统碳、水循环相关的生态系统功能和过程的新视角。随着天空地一体化观测技术的完善以及SIF机理研究的推进, SIF遥感在生态学领域也出现了一些有前景的应用(图3)。

3.3.1 陆地生态系统碳水循环的日变化监测

现有卫星SIF数据受限于时间分辨率和过境时间, 只能监测一天中的某个瞬时。例如GOME-2的9:30, TROPOMI的13:30等。然而, 气温、光照、大气水分、土壤湿度和叶水势都会在一天内发生变化, 进而导致气孔导度、光合作用和蒸腾作用在一天内都发生变化。最近搭载在国际空间站的OCO-3以及未来计划发射的GeoCarb将有望提供基于SIF的植物光合作用和蒸腾作用的昼夜节律(Xiao *et al*., 2021)。此外, 这些地球静止卫星、极轨卫星和地面观测网络协同使用, 将极大地促进我们对陆地生态系统碳水循环的认识。

3.3.2 生物多样性监测

生物多样性是生物(动物、植物、微生物)与环境形成的生态复合体以及与此相关的各种生态过程的总和, 包括生态系统、物种和基因3个层次(马克平, 1993)。生物多样性是生态系统维持稳定的一项重要指标。植物功能多样性是生物多样性概念的基本组成单位, 表征群落内植物个体间功能性状的变异性, 通常群落的功能多样性越高, 则物种多样性也越高(Díaz & Cabido, 2001)。准确量化植被功能多样性的空间分布是遥感反演植物物种多样性的重要途径(Cavender-Bares *et al*., 2022)。近年来, 多源遥感数据(多光谱、高光谱、激光雷达和热红外等)为植物物种多样性的研究与保护工作提供了数据支撑(郭庆华等, 2020)。

SIF与叶片叶绿素含量、叶片氮含量等植物功能性状联系密切(详见**2.1**部分)。因此SIF有望成为跨生态系统和景观尺度表征植物功能多样性的重要的新变量。可以利用SIF反演群落内功能多样性的时空变化, 进而实现植物多样性的动态监测。目前, 已有研究证明将机载高空间分辨率SIF数据与信息论方法相结合可以准确反演植物物种和功能多样性的空间分布(Pacheco-Labrador *et al*., 2019; Tagliabue *et al*., 2020)。未来FLEX高空间分辨率的卫星和机载SIF数据的出现, 结合激光雷达、热红外和微波植被光学厚度等数据, 将会进一步促进我们在跨生态系统和景观尺度准确反演物种多样性和功能多样性的空间格局和时间动态。与此同时, 针对热带雨林、高寒山地等野外观测较为困难的生态系统, SIF遥感可以为物种多样性保护策略提供准确可靠的数据和技术支撑。

3.3.3 空间生态学

空间生态学是研究空间在种群和种间动态中的作用的科学(Legendre & Fortin, 1989)。最近几十年, 受益于地理信息系统和遥感图像技术的发展, 空间趋势分析逐渐被应用于景观尺度上的干扰(例如火灾、虫害和极端天气)和入侵物种等研究(Rietkerk & van de Koppel, 2008)。苛养木杆菌(*Xylella fastidiosa*)

DOI: 10.17521/cjpe.2022.0233

是可以感染超过550种植物的病原体, 入侵到一些欧洲国家后, 对橄榄(*Canarium album*)和欧洲李(*Prunus domestica*)造成毁灭性伤害, 带来严重经济和环境后果。Zarco-Tejada等(2021)使用机载成像高光谱获取超过100万株受感染和健康的树木, 研究表明通过SIF等遥感参数可以监测到病害对橄榄林胁迫状况的空间分布及早期预警。Tang等(2022)使用GOSIF产品分析了2001–2016年全球喀斯特生态系统植被生产力的空间模式和变化趋势, 发现全球大部分喀斯特地区在变绿, 中国变绿空间区域占比78%, 对全球喀斯特生态系统植被生产力恢复起到主导作用。2019到2020年初, 澳大利亚东南地区遭遇了多年干旱和创纪录的高温, 并且发生了特大森林火灾, Qin等(2022)使用星载SIF和植被指数数据、热红外和微波遥感影像评估该森林地区的植被结构和生物量从损失到恢复的变化幅度和速度。未来, 结合植物功能多样性监测, SIF遥感有望更好地服务于空间生态学研究。

3.3.4 光合作用立体监测

植物光合作用监测可以通过红外气体分析仪(例如LI-6400或者LI-6800等)测量叶片或者整个植株的光合作用, 也可以使用涡度协方差(EC)方法测量生态系统尺度的光合作用(Baldocchi, 2003)。然而, 这些方法缺乏空间信息。随着成像SIF遥感的出现, 可结合EC通量测量和LI-6800测量, 揭示生态系统EC测量足迹范围内光合作用的变异性, 进而促进研究微环境、林下和垂直冠层结构的影响, 及生态系统内生物多样性与功能多样性之间的相互作用(Porcar-Castell *et al*., 2021)。此外, 结合LiDAR点云数据, 模拟植被冠层PAR的三维分布, 耦合叶片和冠层辐射传输模型, 可以建立植被冠层SIF三维分布, 从而获取植物的三维光合作用速率(Liu *et al*., 2019a)。随着三维植被荧光辐射传输模型, 例如DART (Gastellu-Etchegorry *et al*., 2017), FluorFLIGHT (Hernández-Clemente *et al*., 2017), FluorWPS (Zhao *et al*., 2022b), FluorRTER (Zeng *et al*., 2020)等模型的不断发展, 未来通过SIF成像、三维SIF辐射传输模型与LiDAR、EC通量等技术相结合, 植被光合作用监测有望实现从平面到立体的转变。

3.3.5 植物生理表型

植物形态性状(株高、叶面积、冠幅、胸径等)的时空变化已被广泛研究, 并用于表征植物受胁迫后的响应(Su *et al*., 2019; Jin *et al*., 2021)。然而, 这些性状不足以捕获植物生理的快速变化。目前, 基于SIF的植物生理表型监测处于早期阶段, 且尚未实现与形态性状表型的同步观测。新兴的SIF成像系统逐渐被应用到精准农业和果树的病虫害监测(Pinto *et al*., 2016; Zarco-Tejada *et al*., 2021)。随着SIF的植物生理信息提取方法和技术的推进, 植物生理表型将更好地服务于精准农林业管理、胁迫早期可视化预警等。

4 总结

本文综述了SIF遥感的基本原理、观测技术及反演算法, 调研了SIF遥感在陆地生态系统功能和过程监测中的应用现状, 并对天空地一体化SIF观测、基于SIF的生理信息提取及SIF遥感的生态学应用3个方面进行了深入讨论和展望。基于上述综述和展望内容, 我们总结了目前SIF遥感面临的问题与挑战:

(1)如何更好地观测SIF? 需要建立覆盖更多植被类型的标准化地面SIF观测网络。然而, 目前不同SIF观测系统间的仪器配置、采集流程、观测方法和反演算法往往存在差异。因此需要进行标准化测量、统一校准协议、光谱质量数据控制, 评估这些因素所造成的不确定性。同时, 机载和无人机SIF观测仍处于早期发展阶段, 一些技术难点需要去攻克。例如, 大气校正、载荷集成、空间定位、飞行成本等。因此需要研发更加方便、快捷、易用的无人机SIF系统, 及更轻便且高质量的成像超高光谱传感器。目前, 低时空分辨率限制了卫星SIF数据在精细尺度的应用, 未来, FLEX、TanSat-2和GeoCarb等新卫星将提高卫星SIF数据的时空分辨率。然而不同传感器观测的SIF波段和数据质量有一定差异。另外地球静止卫星观测角度和太阳高度角对SIF的影响不容忽视。因此, 需要更多的近地SIF观测和模型模拟工作来校准、验证和预演星载SIF数据。

(2)如何准确地解译SIF数据? 遥感获取的冠层SIF数据包含着生理与非生理信息, 如何拆分冠层SIF数据的生理与非生理信息, 以提取准确的植物生理信息, 进而避免不恰当使用冠层SIF而对潜在生态过程产生偏颇的理解, 尚需更深入的研究。目前, FRSIF的生理与非生理信息的解译已经较为成熟, 然而, RSIF的生理信息提取依然是有待解决的

难题。此外, PSI和PSII的能量分配及激发的SIF比例也是有待深入探讨的问题。

(3)如何更广泛地应用SIF? SIF遥感已经提供了全球尺度监测陆地生态系统碳、水循环相关的生态系统功能和过程的新视角。然而, 伴随着天空地一体化观测的发展, 以及SIF机理和模型研究的进展, SIF遥感在生态学领域的应用将更广泛, 有更多的应用领域等待研究者去探索。例如, 目前SIF遥感多着重于陆地生态系统的研究, 未来可关注在海洋藻类、海陆交界的潮间带植被等领域的应用。在胁迫监测上, 目前SIF着重于非生物胁迫的研究, 未来可以拓展在生物胁迫的研究应用(入侵植物胁迫等)。

致谢 感谢南京大学国际地球系统科学研究所曹若臣和赖耕科在文稿撰写工作中给予的帮助。

参考文献

Ač A, Malenovský Z, Olejníčková J, Gallé A, Rascher U, Mohammed G (2015). Meta-analysis assessing potential of steady-state chlorophyll fluorescence for remote sensing detection of plant water, temperature and nitrogen stress. *Remote Sensing of Environment,* 168, 420-436.

Alemohammad SH, Fang B, Konings AG, Aires F, Green JK, Kolassa J, Miralles D, Prigent C, Gentine P (2017). Water, energy, and carbon with Artificial Neural Networks (WECANN): a statistically-based estimate of global surface turbulent fluxes and gross primary productivity using solar-induced fluorescence. *Biogeosciences,* 14, 4101-4124.

Alonso L, Gomez-Chova L, Vila-Frances J, Amoros-Lopez J, Guanter L, Calpe J, Moreno J (2008). Improved Fraunhofer line discrimination method for vegetation fluorescence quantification. *IEEE Geoscience and Remote Sensing Letters,* 5, 620-624.

Alonso L, Gómez-Chova L, Vila-Francés J, Amorós-López J, Guanter L, Calpe J, Moreno J (2007). Sensitivity analysis of the Fraunhofer line discrimination method for the measurement of chlorophyll fluorescence using a field spectroradiometer//IEEE. *2007 IEEE International Geoscience and Remote Sensing Symposium.* IEEE, Barcelona, Spain.

Anav A, Friedlingstein P, Beer C, Ciais P, Harper A, Jones C, Murray-Tortarolo G, Papale D, Parazoo NC, Peylin P, Piao S, Sitch S, Viovy N, Wiltshire A, Zhao M (2015). Spatiotemporal patterns of terrestrial gross primary production: a review. *Reviews of Geophysics,* 53, 785-818.

Atherton J, MacArthur A, Hakala T, Maseyk K, Robinson I, Liu W, Honkavaara E, Porcar-Castell A, IEEE (2018). Drone measurements of solar-induced chlorophyll fluorescence acquired with a low-weight DFOV spectrometer system//IEEE. *2018 IEEE International Geoscience and Remote Sensing Symposium.* IEEE, Valencia, Spain.

Baker NR (2008). Chlorophyll fluorescence: a probe of photosynthesis *in vivo. Annual Review of Plant Biology,* 5, 89-113.

Baldocchi DD (2003). Assessing the eddy covariance technique for evaluating carbon dioxide exchange rates of ecosystems: past, present and future. *Global Change Biology,* 9, 479-492.

Belwalkar A, Poblete T, Longmire A, Hornero A, Hernandez-Clemente R, Zarco-Tejada PJ (2022). Evaluation of SIF retrievals from narrow-band and sub-nanometer airborne hyperspectral imagers flown in tandem: modelling and validation in the context of plant phenotyping. *Remote Sensing of Environment,* 273, 112986. DOI: 10.1016/j.rse.2022.112986.

Bendig J, Malenovský Z, Gautam D, Lucieer A (2020). Solar-induced chlorophyll fluorescence measured from an unmanned aircraft system: sensor etaloning and platform motion correction. *IEEE Transactions on Geoscience and Remote Sensing,* 58, 3437-3444.

Berger K, Verrelst J, Féret JB, Wang ZH, Wocher M, Strathmann M, Danner M, Mauser W, Hank T (2020). Crop nitrogen monitoring: recent progress and principal developments in the context of imaging spectroscopy missions. *Remote Sensing of Environment,* 242, 111758. DOI: 10.1016/j.rse.2020.111758.

Berry J, Bjorkman O (1980). Photosynthetic response and adaptation to temperature in higher plants. *Annual Review of Plant Physiology,* 31, 491-543.

Berry JA, Beerling DJ, Franks PJ (2010). Stomata: key players in the earth system, past and present. *Current Opinion in Plant Biology,* 13, 233-240.

Bertani G, Wagner F, Anderson L, Aragão L (2017). Chlorophyll fluorescence data reveals climate-related photosynthesis seasonality in Amazonian forests. *Remote Sensing,* 9, 1275. DOI: 10.3390/rs9121275.

Biriukova K, Pacheco-Labrador J, Migliavacca M, Mahecha MD, Gonzalez-Cascon R, Martín MP, Rossini M (2021). Performance of singular spectrum analysis in separating seasonal and fast physiological dynamics of solar-induced chlorophyll fluorescence and PRI optical signals. *Journal of Geophysical Research: Biogeosciences,* 126, e2020JG006158. DOI: 10.1029/2020JG006158.

Breshears DD, Cobb NS, Rich PM, Price KP, Allen CD, Balice RG, Romme WH, Kastens JH, Floyd ML, Belnap J, Anderson JJ, Myers OB, Meyer CW (2005). Regional vegetation die-off in response to global-change-type drought. *Proceedings of the National Academy of Sciences of the United States of America,* 102, 15144-15148.

DOI: 10.17521/cjpe.2022.0233

Buman B, Hueni A, Colombo R, Cogliati S, Celesti M, Julitta T, Burkart A, Siegmann B, Rascher U, Drusch M, Damm A (2022). Towards consistent assessments of *in situ* radiometric measurements for the validation of fluorescence satellite missions. *Remote Sensing of Environment,* 274, 112984. DOI: 10.1016/j.rse.2022.112984.

Burkart A, Schickling A, Mateo MPC, Wrobel TJ, Rossini M, Cogliati S, Julitta T, Rascher U (2015). A method for uncertainty assessment of passive sun-induced chlorophyll fluorescence retrieval using an infrared reference light. *IEEE Sensors Journal,* 15, 4603-4611.

Camino C, González-Dugo V, Hernández P, Sillero JC, Zarco-Tejada PJ (2018). Improved nitrogen retrievals with airborne-derived fluorescence and plant traits quantified from VNIR-SWIR hyperspectral imagery in the context of precision agriculture. *International Journal of Applied Earth Observation and Geoinformation,* 70, 105-117.

Camino C, Gonzalez-Dugo V, Hernandez P, Zarco-Tejada PJ (2019). Radiative transfer *V*cmax estimation from hyperspectral imagery and SIF retrievals to assess photosynthetic performance in rainfed and irrigated plant phenotyping trials. *Remote Sensing of Environment,* 231, 111186. DOI: 10.1016/j.rse.2019.05.005.

Cavender-Bares J, Schneider FD, Santos MJ, Armstrong A, Carnaval A, Dahlin KM, Fatoyinbo L, Hurtt GC, Schimel D, Townsend PA, Ustin SL, Wang ZH, Wilson, AM (2022). Integrating remote sensing with ecology and evolution to advance biodiversity conservation. *Nature Ecology & Evolution,* 6, 506-519.

Celesti M, van der Tol C, Cogliati S, Panigada C, Yang PQ, Pinto F, Rascher U, Miglietta F, Colombo R, Rossini M (2018). Exploring the physiological information of Sun-induced chlorophyll fluorescence through radiative transfer model inversion. *Remote Sensing of Environment,* 215, 97-108.

Chambers JQ, Asner GP, Morton DC, Anderson LO, Saatchi SS, Espírito-Santo FD, Palace M, Souza Jr C (2007). Regional ecosystem structure and function: ecological insights from remote sensing of tropical forests. *Trends in Ecology & Evolution,* 22, 414-423.

Chang CY, Wen JM, Han JM, Kira O, LeVonne J, Melkonian J, Riha SJ, Skovira J, Ng S, Gu LH, Wood JD, Näthe P, Sun Y (2021). Unpacking the drivers of diurnal dynamics of sun-induced chlorophyll fluorescence (SIF): canopy structure, plant physiology, instrument configuration and retrieval methods. *Remote Sensing of Environment,* 265, 112672. DOI: 10.1016/j.rse.2021.112672.

Chang CY, Zhou RQ, Kira O, Marri S, Skovira J, Gu LH, Sun Y (2020). An Unmanned Aerial System (UAS) for concurrent measurements of solar-induced chlorophyll fluorescence and hyperspectral reflectance toward improving crop monitoring. *Agricultural and Forest Meteorology,* 294, 108145. DOI: 10.1016/j.agrformet.2020.108145.

Chapin F, Matson P, Mooney H (2002). *Principles of Terrestrial Ecosystem Ecology.* 2nd ed. Springer, New York.

Chen JD, Liu XJ, Du SS, Ma Y, Liu LY (2021). Effects of drought on the relationship between photosynthesis and chlorophyll fluorescence for maize. *IEEE Journal of Selected Topics in Applied Earth Observations and Remote Sensing,* 14, 11148-11161.

Cogliati S, Rossini M, Julitta T, Meroni M, Schickling A, Burkart A, Pinto F, Rascher U, Colombo R (2015a). Continuous and long-term measurements of reflectance and sun-induced chlorophyll fluorescence by using novel automated field spectroscopy systems. *Remote Sensing of Environment,* 164, 270-281.

Cogliati S, Verhoef W, Kraft S, Sabater N, Alonso L, Vicent J, Moreno J, Drusch M, Colombo R (2015b). Retrieval of sun-induced fluorescence using advanced spectral fitting methods. *Remote Sensing of Environment,* 169, 344-357.

Colombo R, Celesti M, Bianchi RM, Campbell PKE, Cogliati S, Cook BD, Corp LA, Damm A, Domec JC, Guanter L, Julitta T, Middleton EM, Noormets A, Panigada C, Pinto F, *et al.* (2018). Variability of sun-induced chlorophyll fluorescence according to stand age-related processes in a managed loblolly pine forest. *Global Change Biology,* 24, 2980-2996.

Coppo P, Taiti A, Pettinato L, Francois M, Taccola M, Drusch M (2017). Fluorescence imaging spectrometer (FLORIS) for ESA FLEX mission. *Remote Sensing,* 9, 649. DOI: 10.3390/rs9070649.

Corp L, Middleton E, Daughtry C, Campbell P (2006). Solar induced fluorescence and reflectance sensing techniques for monitoring nitrogen utilization in corn//IEEE. *2006 IEEE International Symposium on Geoscience and Remote Sensing.* IEEE, Denver, USA. 2267-2270.

Croft H, Chen JM, Wang R, Mo G, Luo S, Luo X, He L, Gonsamo A, Arabian J, Zhang Y, Simic-Milas A, Noland TL, He Y, Homolová L, Malenovský Z, *et al.* (2020). The global distribution of leaf chlorophyll content. *Remote Sensing of Environment,* 236, 111479. DOI: 10.1016/j.rse.2019.111479.

Culpepper AS, York AC (1999). Weed management in glufosinate-resistant corn (*Zea mays*). *Weed Technology,* 13, 324-333.

Damm A, Cogliati S, Colombo R, Fritsche L, Genangeli A, Genesio L, Hanus J, Peressotti A, Rademske P, Rascher U, Schuettemeyer D, Siegmann B, Sturm J, Miglietta F (2022). Response times of remote sensing measured sun-induced chlorophyll fluorescence, surface temperature and vegetation indices to evolving soil water limitation in a crop canopy. *Remote Sensing of Environment,* 273,

112957. DOI: 10.1016/j.rse.2022.112957.

Damm A, Elber J, Erler A, Gioli B, Hamdi K, Hutjes R, Kosvancova M, Meroni M, Miglietta F, Moersch A, Moreno J, Schickling A, Sonnenschein R, Udelhoven T, van der Linden S, *et al.* (2010). Remote sensing of sun-induced fluorescence to improve modeling of diurnal courses of gross primary production (GPP). *Global Change Biology,* 16, 171-186.

Damm A, Guanter L, Laurent VCE, Schaepman ME, Schickling A, Rascher U (2014). FLD-based retrieval of sun-induced chlorophyll fluorescence from medium spectral resolution airborne spectroscopy data. *Remote Sensing of Environment,* 147, 256-266.

Damm A, Guanter L, Paul-Limoges E, van der Tol C, Hueni A, Buchmann N, Eugster W, Ammann C, Schaepman ME (2015). Far-red sun-induced chlorophyll fluorescence shows ecosystem-specific relationships to gross primary production: an assessment based on observational and modeling approaches. *Remote Sensing of Environment,* 166, 91-105.

Damm A, Haghighi E, Paul-Limoges E, van der Tol C (2021). On the seasonal relation of sun-induced chlorophyll fluorescence and transpiration in a temperate mixed forest. *Agricultural and Forest Meteorology,* 304-305, 108386. DOI: 10.1016/j.agrformet.2021.108386.

Damm A, Roethlin S, Fritsche L (2018). Towards advanced retrievals of plant transpiration using sun-induced chlorophyll fluorescence: first considerations//IEEE. *2018 IEEE International Geoscience and Remote Sensing Symposium.* IEEE, Valencia, Spain. 5983-5986.

Dannenberg M, Wang X, Yan D, Smith W (2020). Phenological characteristics of global ecosystems based on optical, fluorescence, and microwave remote sensing. *Remote Sensing,* 12, 671. DOI: 10.3390/rs12040671.

Daumard F, Champagne S, Fournier A, Goulas Y, Ounis A, Hanocq JF, Moya I (2010). A field platform for continuous measurement of canopy fluorescence. *IEEE Transactions on Geoscience and Remote Sensing,* 48, 3358-3368.

Daumard F, Goulas Y, Champagne S, Fournier A, Ounis A, Olioso A, Moya I (2012). Continuous monitoring of canopy level sun-induced chlorophyll fluorescence during the growth of a sorghum field. *IEEE Transactions on Geoscience and Remote Sensing,* 50, 4292-4300.

Díaz S, Cabido M (2001). Vive la différence: plant functional diversity matters to ecosystem processes. *Trends in Ecology & Evolution,* 16, 646-655.

Dobrowski SZ, Pushnik JC, Zarco-Tejada PJ, Ustin SL (2005). Simple reflectance indices track heat and water stress-induced changes in steady-state chlorophyll fluorescence at the canopy scale. *Remote Sensing of Environment,* 97, 403-414.

Doughty R, Köhler P, Frankenberg C, Magney TS, Xiao XM, Qin YW, Wu XC, Moore III B (2019). TROPOMI reveals dry-season increase of solar-induced chlorophyll fluorescence in the Amazon forest. *Proceedings of the National Academy of Sciences of the United States of America,* 116, 22393-22398.

Drusch M, Moreno J, del Bello U, Franco R, Goulas Y, Huth A, Kraft S, Middleton EM, Miglietta F, Mohammed G, Nedbal L, Rascher U, Schüttemeyer D, Verhoef W (2017). The FLuorescence EXplorer mission concept—ESA's earth explorer 8. *IEEE Transactions on Geoscience and Remote Sensing,* 55, 1273-1284.

Du SS, Liu LY, Liu XJ, Guo J, Hu JC, Wang SQ, Zhang YG (2019). SIFSpec: measuring solar-induced chlorophyll fluorescence observations for remote sensing of photosynthesis. *Sensors,* 19, 3009. DOI: 10.3390/s19133009.

Du SS, Liu LY, Liu XJ, Zhang X, Zhang XY, Bi YM, Zhang LC (2018). Retrieval of global terrestrial solar-induced chlorophyll fluorescence from TanSat satellite. *Science Bulletin,* 63, 1502-1512.

Duveiller G, Filipponi F, Walther S, Köhler P, Frankenberg C, Guanter L, Cescatti A (2020). A spatially downscaled Sun-induced fluorescence global product for enhanced monitoring of vegetation productivity. *Earth System Science Data,* 12, 1101-1116.

Evans JR (1989). Photosynthesis and nitrogen relationships in leaves of C_3 plants. *Oecologia,* 78, 9-19.

Field CB, Randerson JT, Malmström CM (1995). Global net primary production: combining ecology and remote sensing. *Remote Sensing of Environment,* 51, 74-88.

Fisher JB, Melton F, Middleton E, Hain C, Anderson MC, Allen R, McCabe M, Hook S, Baldocchi D, Townsend P, Kilic A, Tu K, Miralles DD, Perret J, Lagouarde J, *et al.* (2017). The future of evapotranspiration: global requirements for ecosystem functioning, carbon and climate feedbacks, agricultural management, and water resources. *Water Resources Research,* 53, 2618-2626.

Fournier A, Daumard F, Champagne S, Ounis A, Goulas Y, Moya I (2012). Effect of canopy structure on sun-induced chlorophyll fluorescence. *ISPRS Journal of Photogrammetry and Remote Sensing,* 68, 112-120.

Frankenberg C, Fisher J, Worden J, Badgley G, Saatchi S, Lee J, Toon G, Butz A, Jung M, Kuze A, Yokota T (2011). New global observations of the terrestrial carbon cycle from GOSAT: patterns of plant fluorescence with gross primary productivity. *Geophysical Research Letters,* 38. L17706. DOI: 10.1029/2011GL048738.

Frankenberg C, Köhler P, Magney TS, Geier S, Lawson P, Schwochert M, McDuffie J, Drewry DT, Pavlick R, Kuhnert A (2018). The Chlorophyll Fluorescence Imaging Spectrometer (CFIS), mapping far red fluorescence from aircraft. *Remote Sensing of Environment,* 217, 523-536.

DOI: 10.17521/cjpe.2022.0233

Freedman A, Cavender-Bares J, Kebabian P, Bhaskar R, Scott H, Bazzaz F (2002). Remote sensing of solar-excited plant fluorescence as a measure of photosynthetic rate. *Photosynthetica,* 40, 127-132.

Fu P, Meacham-Hensold K, Siebers MH, Bernacchi CJ (2020). The inverse relationship between solar-induced fluorescence yield and photosynthetic capacity: benefits for field phenotyping. *Journal of Experimental Botany,* 72, 1295-1306.

Garzonio R, Colombo R, Cogliati S, Mauro BD (2017). Surface reflectance and Sun-induced fluorescence spectroscopy measurements using a small hyperspectral UAS. *Remote Sensing,* 9, 472. DOI: 10.3390/rs9050472.

Gastellu-Etchegorry JP, Lauret N, Yin TG, Landier L, Kallel A, Malenovský Z, Bitar AA, Aval J, Benhmida S, Qi JB, Medjdoub G, Guilleux J, Chavanon E, Cook B, Morton D, *et al.* (2017). DART: recent advances in remote sensing data modeling with atmosphere, polarization, and chlorophyll fluorescence. *IEEE Journal of Selected Topics in Applied Earth Observations and Remote Sensing,* 10, 2640-2649.

Gautam D, Lucieer A, Bendig J, Malenovský Z (2020). Footprint determination of a spectroradiometer mounted on an unmanned aircraft system. *IEEE Transactions on Geoscience and Remote Sensing,* 58, 3085-3096.

Ge QS, Dai JH, Zheng JY (2010). The progress of phenology studies and challenges to modern phenology research in China. *Bulletin of Chinese Academy of Sciences,* 25, 310-316. [葛全胜, 戴君虎, 郑景云 (2010). 物候学研究进展及中国现代物候学面临的挑战. 中国科学院院刊, 25, 310-316.]

Gentine P, Alemohammad SH (2018). Reconstructed solar-induced fluorescence: a machine learning vegetation product based on MODIS surface reflectance to reproduce GOME-2 solar-induced fluorescence. *Geophysical Research Letters,* 45, 3136-3146.

Gensheimer J, Turner AJ, Köhler P, Frankenberg C, Chen J (2022). A convolutional neural network for spatial downscaling of satellite-based solar-induced chlorophyll fluorescence (SIFnet). *Biogeosciences,* 19, 1777-1793.

Gerhards M, Schlerf M, Rascher U, Udelhoven T, Juszczak R, Alberti G, Miglietta F, Inoue Y (2018). Analysis of airborne optical and thermal imagery for detection of water stress symptoms. *Remote Sensing,* 10, 1139. DOI: 10.3390/rs10071139.

Gitelson AA, Buschmann C, Lichtenthaler HK (1998). Leaf chlorophyll fluorescence corrected for re-absorption by means of absorption and reflectance measurements. *Journal of Plant Physiology,* 152, 283-296.

Gitelson AA, Viña A, Ciganda V, Rundquist DC, Arkebauer TJ (2005). Remote estimation of canopy chlorophyll content in crops. *Geophysical Research Letters,* 32, 1-4.

GomezChova L, AlonsoChorda L, Lopez JA, Frances JV, del ValleTascon S, Calpe J, Moreno J (2006). Solar induced fluorescence measurements using a field spectroradiometer// AIP. *AIP Conference Proceedings.* AIP, Cairo, Egypt. 274-281.

Goulas Y, Fournier A, Daumard F, Champagne S, Ounis A, Marloie O, Moya I (2017). Gross primary production of a wheat canopy relates stronger to far red than to red solar-induced chlorophyll fluorescence. *Remote Sensing,* 9, 97. DOI: 10.3390/rs9010097.

Grace J, Nichol C, Disney M, Lewis P, Quaife T, Bowyer P (2007). Can we measure terrestrial photosynthesis from space directly, using spectral reflectance and fluorescence? *Global Change Biology,* 13, 1484-1497.

Grossmann K, Frankenberg C, Magney TS, Hurlock SC, Seibt U, Stutz J (2018). PhotoSpec: a new instrument to measure spatially distributed red and far-red Solar-Induced Chlorophyll Fluorescence. *Remote Sensing of Environment,* 216, 311-327.

Gu L, Wood J, Chang CY, Sun Y, Riggs J (2019). Advancing terrestrial ecosystem science with a novel automated measurement system for sun-induced chlorophyll fluorescence for integration with eddy covariance flux networks. *Journal of Geophysical Research: Biogeosciences,* 124, 127-146.

Guanter L, Alonso L, Gómez-Chova L, Amorós-López J, Vila J, Moreno J (2007). Estimation of solar-induced vegetation fluorescence from space measurements. *Geophysical Research Letters,* 34, L08401. DOI: 10.1029/2007GL029289.

Guanter L, Alonso L, Gómez-Chova L, Meroni M, Preusker R, Fischer J, Moreno J (2010). Developments for vegetation fluorescence retrieval from spaceborne high-resolution spectrometry in the O_2-A and O_2-B absorption bands. *Journal of Geophysical Research, Atmospheres,* 115, D19303. DOI: 10.1029/2009JD013716.

Guanter L, Bacour C, Schneider A, Aben I, van Kempen T, Maignan F, Retscher C, Köhler P, Frankenberg C, Joiner J, Zhang Y (2021). The TROPOSIF global sun-induced fluorescence dataset from the Sentinel-5P TROPOMI mission. *Earth System Science Data,* 13, 5423-5440.

Guanter L, Frankenberg C, Dudhia A, Lewis PE, Gómez-Dans J, Kuze A, Suto H, Grainger RG (2012). Retrieval and global assessment of terrestrial chlorophyll fluorescence from GOSAT space measurements. *Remote Sensing of Environment,* 121, 236-251.

Guanter L, Rossini M, Colombo R, Meroni M, Frankenberg C, Lee JE, Joiner J (2013). Using field spectroscopy to assess the potential of statistical approaches for the retrieval of sun-induced chlorophyll fluorescence from ground and space. *Remote Sensing of Environment,* 133, 52-61.

Guanter L, Zhang YG, Jung M, Joiner J, Voigt M, Berry JA,

Frankenberg C, Huete AR, Zarco-Tejada P, Lee JE, Moran MS, Ponce-Campos G, Beer C, Camps-Valls G, Buchmann N, *et al.* (2014). Global and time-resolved monitoring of crop photosynthesis with chlorophyll fluorescence. *Proceedings of the National Academy of Sciences of the United States of America,* 111, E1327-E1333.

Guo QH, Hu TY, Ma Q, Xu KX, Yang QL, Sun QH, Li YM, Su YJ (2020). Advances for the new remote sensing technology in ecosystem ecology research. *Chinese Journal of Plant Ecology,* 44, 418-435. [郭庆华, 胡天宇, 马勤, 徐可心, 杨秋丽, 孙千惠, 李玉美, 苏艳军 (2020). 新一代遥感技术助力生态系统生态学研究. 植物生态学报, 44, 418-435.]

Han JM, Chang CYY, Gu LH, Zhang YJ, Meeker EW, Magney TS, Walker AP, Wen JM, Kira O, McNaull S, Sun Y (2022a). The physiological basis for estimating photosynthesis from Chla fluorescence. *New Phytologist,* 234, 1206-1219.

Han JM, Gu LH, Wen JM, Sun Y (2022b). Inference of photosynthetic capacity parameters from chlorophyll a fluorescence is affected by redox state of PSII reaction centers. *Plant, Cell & Environment,* 45, 1298-1314.

Hao D, Asrar G, Zeng YL, Yang X, Li X, Xiao JF, Guan K, Wen JG, Xiao Q, Berry J, Chen M (2021a). Potential of hotspot solar-induced chlorophyll fluorescence for better tracking terrestrial photosynthesis. *Global Change Biology,* 27, 2144-2158.

Hao DL, Zeng YL, Zhang ZY, Zhang YG, Qiu H, Biriukova K, Celesti M, Rossini M, Zhu P, Asrar GR, Chen M (2022). Adjusting solar-induced fluorescence to nadir-viewing provides a better proxy for GPP. *ISPRS Journal of Photogrammetry and Remote Sensing,* 186, 157-169.

Hao DL, Zeng, YL, Qiu H, Biriukova K, Celesti M, Migliavacca M, Rossini M, Asrar GR, Chen M (2021b). Practical approaches for normalizing directional solar-induced fluorescence to a standard viewing geometry. *Remote Sensing of Environment,* 255, 112171. DOI: 10.1016/j.rse.2020.112171.

Helm LT, Shi HY, Lerdau MT, Yang X (2020). Solar-induced chlorophyll fluorescence and short-term photosynthetic response to drought. *Ecological Applications,* 30, e02101. DOI: 10.1002/eap.2101.

Hernández-Clemente R, North PRJ, Hornero A, Zarco-Tejada PJ (2017). Assessing the effects of forest health on sun-induced chlorophyll fluorescence using the FluorFLIGHT 3-D radiative transfer model to account for forest structure. *Remote Sensing of Environment,* 193, 165-179.

Hou P, Yang M, Zhai J, Liu XM, Wan HW, Li J, Cai MY, Liu HM (2017). Discussion about natural reserve and construction of national ecological security pattern. *Geographical Research,* 36, 420-428. [侯鹏, 杨旻, 翟俊, 刘晓曼, 万华伟, 李静, 蔡明勇, 刘慧明 (2017). 论自然保护地与国家生态安全格局构建. 地理研究, 36, 420-428.]

Hu JC, Liu LY, Guo J, Du SS, Liu XJ (2018). Upscaling solar-induced chlorophyll fluorescence from an instantaneous to daily scale gives an improved estimation of the gross primary productivity. *Remote Sensing,* 10, 1663. DOI: 10.3390/rs10101663.

Huang BR, Ma YH, Huang K, Su LY, Zhang CL, Cheng DW, Wang Y (2018). Strategic approach on promoting reform of China's natural protected areas system with National Parks as backbone. *Bulletin of Chinese Academy of Sciences,* 33, 1342-1351. [黄宝荣, 马永欢, 黄凯, 苏利阳, 张丛林, 程多威, 王毅 (2018). 推动以国家公园为主体的自然保护地体系改革的思考. 中国科学院院刊, 33, 1342-1351.]

Huang Y, Zhou C, Du MH, Wu PF, Yuan L, Tang JW (2022). Tidal influence on the relationship between solar-induced chlorophyll fluorescence and canopy photosynthesis in a coastal salt marsh. *Remote Sensing of Environment,* 270, 112865. DOI: 10.1016/j.rse.2021.112865.

Jeong SJ, Schimel D, Frankenberg C, Drewry DT, Fisher JB, Verma M, Berry JA, Lee JE, Joiner J (2017). Application of satellite solar-induced chlorophyll fluorescence to understanding large-scale variations in vegetation phenology and function over northern high latitude forests. *Remote Sensing of Environment,* 190, 178-187.

Ji MH, Tang BH, Li ZL (2019). Review of solar-induced chlorophyll fluorescence retrieval methods from satellite data. *Remote Sensing Technology and Application,* 34, 455-466. [纪梦豪, 唐伯惠, 李召良 (2019). 太阳诱导叶绿素荧光的卫星遥感反演方法研究进展. 遥感技术与应用, 34, 455-466.]

Jia M, Colombo R, Rossini M, Celesti M, Zhu J, Cogliati S, Cheng T, Tian YC, Zhu Y, Cao WX, Yao X (2021). Estimation of leaf nitrogen content and photosynthetic nitrogen use efficiency in wheat using sun-induced chlorophyll fluorescence at the leaf and canopy scales. *European Journal of Agronomy,* 122, 126192. DOI: 10.1016/j.eja.2020.126192.

Jia M, Zhu J, Ma CC, Alonso L, Li D, Cheng T, Tian YC, Zhu Y, Yao X, Cao WX (2018). Difference and potential of the upward and downward sun-induced chlorophyll fluorescence on detecting leaf nitrogen concentration in wheat. *Remote Sensing,* 10, 1315. DOI: 10.3390/rs10081315.

Jin SC, Sun XL, Wu FF, Su YJ, Li YM, Song SL, Xu KX, Ma Q, Baret F, Jiang D, Ding YF, Guo QH (2021). Lidar sheds new light on plant phenomics for plant breeding and management: recent advances and future prospects. *ISPRS Journal of Photogrammetry and Remote Sensing,* 171,

DOI: 10.17521/cjpe.2022.0233

202-223.

Jing X, Bai ZF, Gao Y, Liu LY (2019). Wheat stripe rust monitoring by random forest algorithm combined with SIF and reflectance spectrum. *Transactions of the Chinese Society of Agricultural Engineering,* 35(13), 154-161. [竞霞, 白宗璠, 高媛, 刘良云 (2019). 利用随机森林法协同SIF和反射率光谱监测小麦条锈病. 农业工程学报, 35(13), 154-161.]

Joiner J, Guanter L, Lindstrot R, Voigt M, Vasilkov AP, Middleton EM, Huemmrich KF, Yoshida Y, Frankenberg C (2013). Global monitoring of terrestrial chlorophyll fluorescence from moderate spectral resolution near-infrared satellite measurements: methodology, simulations, and application to GOME-2. *Atmospheric Measurement Techniques Discussions,* 6, 3883-3930. DOI: 10.5194/amt-6-2803-2013.

Joiner J, Yoshida Y, Guanter L, Middleton EM (2016). New methods for retrieval of chlorophyll red fluorescence from hyper-spectral satellite instruments: simulations and application to GOME-2 and SCIAMACHY. *Atmospheric Measurement Techniques Discussions,* 2016, 1-41.

Joiner J, Yoshida Y, Vasilkov AP, Corp LA, Middleton EM (2011). First observations of global and seasonal terrestrial chlorophyll fluorescence from space. *Biogeosciences,* 8, 637-651.

Joiner J, Yoshida Y, Vasilkov AP, Middleton EM, Kuze A, Corp LA (2012). Filling-in of near-infrared solar lines by terrestrial fluorescence and other geophysical effects: simulations and space-based observations from SCIAMACHY and GOSAT. *Atmospheric Measurement Techniques,* 5, 809-829.

Joiner J, Yoshida Y, Vasilkov AP, Schaefer K, Jung M, Guanter L, Zhang Y, Garrity S, Middleton EM, Huemmrich KF, Gu L, Belelli Marchesini L (2014). The seasonal cycle of satellite chlorophyll fluorescence observations and its relationship to vegetation phenology and ecosystem atmosphere carbon exchange. *Remote Sensing of Environment,* 152, 375-391.

Jonard F, de Cannière S, Brüggemann N, Gentine P, Short Gianotti DJ, Lobet G, Miralles DG, Montzka C, Pagán BR, Rascher U, Vereecken H (2020). Value of sun-induced chlorophyll fluorescence for quantifying hydrological states and fluxes: current status and challenges. *Agricultural and Forest Meteorology,* 291, 108088. DOI: 10.1016/j.agrformet.2020.108088.

Julitta T, Burkart A, Colombo R, Rossini M, Schickling A, Migliavacca M, Cogliati S, Wutzler T, Rascher U (2017). Accurate measurements of fluorescence in the O_2A and O_2B band using the FloX spectroscopy system—Results and prospects. [2022-06-06]. http://refhub.elsevier.com/S0168-1923(22)00251-9/sbref0034.

Kimm H, Guan KY, Burroughs CH, Peng B, Ainsworth EA, Bernacchi CJ, Moore CE, Kumagai E, Yang X, Berry JA, Wu GH (2021). Quantifying high-temperature stress on soybean canopy photosynthesis: the unique role of sun-induced chlorophyll fluorescence. *Global Change Biology,* 27, 2403-2415.

Koffi EN, Rayner PJ, Norton AJ, Frankenberg C, Scholze M (2015). Investigating the usefulness of satellite-derived fluorescence data in inferring gross primary productivity within the carbon cycle data assimilation system. *Biogeosciences,* 12, 4067-4084.

Köhler P, Frankenberg C, Magney TS, Guanter L, Joiner J, Landgraf J (2018). Global retrievals of solar induced chlorophyll fluorescence with TROPOMI: first results and inter-sensor comparison to OCO-2. *Geophysical Research Letters,* 45, 10456-10463.

Köhler P, Guanter L, Frankenberg C (2015a). Simplified physically based retrieval of sun-induced chlorophyll fluorescence from GOSAT data. *IEEE Geoscience and Remote Sensing Letters,* 12, 1446-1450.

Köhler P, Guanter L, Joiner J (2015b). A linear method for the retrieval of sun-induced chlorophyll fluorescence from GOME-2 and SCIAMACHY data. *Atmospheric Measurement Techniques,* 8, 2589-2608.

Lee JE, Berry JA, van der Tol C, Yang X, Guanter L, Damm A, Baker I, Frankenberg C (2015). Simulations of chlorophyll fluorescence incorporated into the Community Land Model version 4. *Global Change Biology,* 21, 3469-3477.

Lee JE, Frankenberg C, van der Tol C, Berry JA, Guanter L, Boyce CK, Fisher JB, Morrow E, Worden JR, Asefi S, Badgley G, Saatchi S (2013). Forest productivity and water stress in *Amazonia:* observations from GOSAT chlorophyll fluorescence. *Proceedings of the Royal Society B: Biological Sciences,* 280, 20130171. DOI: 10.1098/rspb.2013.0171.

Legendre P, Fortin MJ (1989). Spatial pattern and ecological analysis. *Vegetatio,* 80, 107-138.

Li J, Zhang YG, Gu LH, Li ZH, Li J, Zhang Q, Zhang ZY, Song L (2020a). Seasonal variations in the relationship between sun-induced chlorophyll fluorescence and photosynthetic capacity from the leaf to canopy level in a rice crop. *Journal of Experimental Botany,* 71, 7179-7197.

Li Q, Zhu JH, Xiao WF (2019). Relationships and trade-offs between, and management of biodiversity and ecosystem services. *Acta Ecologica Sinica,* 39, 2655-2666. [李奇, 朱建华, 肖文发 (2019). 生物多样性与生态系统服务——关系、权衡与管理. 生态学报, 39, 2655-2666.]

Li X, Xiao JF (2019). A global 0.05-degree product of solar-induced chlorophyll fluorescence derived from OCO-2, MODIS, and reanalysis data. *Remote Sensing,* 11, 517. DOI: 10.3390/rs11050517.

Li X, Xiao JF (2022). TROPOMI observations allow for robust exploration of the relationship between solar-induced

chlorophyll fluorescence and terrestrial gross primary production. *Remote Sensing of Environment,* 268, 112748. DOI: 10.1016/j.rse.2021.112748.

Li X, Xiao JF, Kimball JS, Reichle RH, Scott RL, Litvak ME, Bohrer G, Frankenberg C (2020b). Synergistic use of SMAP and OCO-2 data in assessing the responses of ecosystem productivity to the 2018 US drought. *Remote Sensing of Environment,* 251, 112062. DOI: 10.1016/j.rse.2020.112062.

Li ZH, Zhang Q, Li J, Yang X, Wu YF, Zhang ZY, Wang SH, Wang HZ, Zhang YG (2020c). Solar-induced chlorophyll fluorescence and its link to canopy photosynthesis in maize from continuous ground measurements. *Remote Sensing of Environment,* 236, 111420. DOI: 10.1016/j.rse.2019.111420.

Li ZH, Zhang YG, Zhang Q, Wu YF, Zhang XK, Zhang ZY (2021). Tower-based automatic observation methods and systems of solar-induced chlorophyll fluorescence in vegetation canopy. *National Remote Sensing Bulletin,* 25, 1152-1168. [李朝晖, 张永光, 张乾, 吴云飞, 张小康, 章钊颖 (2021). 植被冠层日光诱导叶绿素荧光塔基自动观测方法及系统介绍. 遥感学报, 25, 1152-1168.]

Lichtenthaler HK, Rinderle U (1988). The role of chlorophyll fluorescence in the detection of stress conditions in plants. *CRC Critical Reviews in Analytical Chemistry,* 19, S29-S85.

Liu GH, Wang YS, Chen YN, Tong XQ, Wang YD, Xie J, Tang XG (2022). Remotely monitoring vegetation productivity in two contrasting subtropical forest ecosystems using solar-induced chlorophyll fluorescence. *Remote Sensing,* 14, 1328. DOI: 10.3390/rs14061328.

Liu LY, Chen LF, Liu Y, Yang DX, Zhang XY, Lu NM, Ju WM, Jiang F, Yin ZS, Liu GH, Tian LF, Hu DH, Mao HQ, Liu SH, Zhang JH, *et al.* (2022). Satellite remote sensing for global stocktaking: methods, progress and perspectives. *National Remote Sensing Bulletin,* 26, 243-267. [刘良云, 陈良富, 刘毅, 杨东旭, 张兴赢, 卢乃锰, 居为民, 江飞, 尹增山, 刘国华, 田龙飞, 胡登辉, 毛慧琴, 刘思含, 张建辉, 等 (2022). 全球碳盘点卫星遥感监测方法、进展与挑战. 遥感学报, 26, 243-267.]

Liu LY, Cheng ZH (2010). Detection of vegetation light-use efficiency based on solar-induced chlorophyll fluorescence separated from canopy radiance spectrum. *IEEE Journal of Selected Topics in Applied Earth Observations and Remote Sensing,* 3, 306-312.

Liu LY, Guan LL, Liu XJ (2017). Directly estimating diurnal changes in GPP for C_3 and C_4 crops using far-red sun-induced chlorophyll fluorescence. *Agricultural and Forest Meteorology,* 232, 1-9.

Liu LY, Zhang YJ, Jiao QJ, Peng DL (2013a). Assessing photosynthetic light-use efficiency using a solar-induced chlorophyll fluorescence and photochemical reflectance index. *International Journal of Remote Sensing,* 34, 4264-4280.

Liu LY, Zhao JJ, Guan LL (2013b). Tracking photosynthetic injury of paraquat-treated crop using chlorophyll fluorescence from hyperspectral data. *European Journal of Remote Sensing,* 46, 459-473.

Liu LZ, Teng YG, Wu JJ, Zhao WH, Liu SS, Shen Q (2020a). Soil water deficit promotes the effect of atmospheric water deficit on solar-induced chlorophyll fluorescence. *Science of the Total Environment,* 720, 137408. DOI: 10.1016/j.scitotenv.2020.137408.

Liu WW, Atherton J, Mõttus M, Gastellu-Etchegorry JP, Malenovský Z, Raumonen P, Åkerblom M, Mäkipää R, Porcar-Castell A (2019a). Simulating solar-induced chlorophyll fluorescence in a boreal forest stand reconstructed from terrestrial laser scanning measurements. *Remote Sensing of Environment,* 232, 111274. DOI: 10.1016/j.rse.2019.111274.

Liu X, Guo J, Hu J, Liu L (2019b). Atmospheric correction for tower-based solar-induced chlorophyll fluorescence observations at O_2-A band. *Remote Sensing,* 11, 355. DOI: 10.3390/rs11030355.

Liu XJ, Guanter L, Liu LY, Damm A, Malenovský Z, Rascher U, Peng DL, Du SS, Gastellu-Etchegorry JP (2019c). Downscaling of solar-induced chlorophyll fluorescence from canopy level to photosystem level using a random forest model. *Remote Sensing of Environment,* 231, 110772. DOI: 10.1016/j.rse.2018.05.035.

Liu XJ, Liu LY (2015). Improving chlorophyll fluorescence retrieval using reflectance reconstruction based on principal components analysis. *IEEE Geoscience and Remote Sensing Letters,* 12, 1645-1649.

Liu XJ, Liu LY, Hu JC, Guo J, Du SS (2020b). Improving the potential of red SIF for estimating GPP by downscaling from the canopy level to the photosystem level. *Agricultural and Forest Meteorology,* 281, 107846. DOI: 10.1016/j.agrformet.2019.107846.

Liu XJ, Liu LY, Zhang S, Zhou XF (2015). New spectral fitting method for full-spectrum solar-induced chlorophyll fluorescence retrieval based on principal components analysis. *Remote Sensing,* 7, 10626-10645.

Liu XT, Zhou L, Shi H, Wang SQ, Chi YG (2018). Phenological characteristics of temperate coniferous and broad-leaved mixed forests based on multiple remote sensing vegetation indices, chlorophyll fluorescence and CO_2 flux data. *Acta Ecologica Sinica,* 38, 3482-3494. [刘啸添, 周蕾, 石浩, 王绍强, 迟永刚 (2018). 基于多种遥感植被指数、叶绿素荧光与CO_2通量数据的温带针阔混交林物候特征对比分析. 生态学报, 38, 3482-3494.]

Liu YJ, You CH, Zhang YG, Chen SP, Zhang ZY, Li J, Wu YF (2021). Resistance and resilience of grasslands to drought

detected by SIF in Inner Mongolia, China. *Agricultural and Forest Meteorology,* 308-309, 108567. DOI: 10.1016/j.agrformet.2021.108567.

Lu XL, Liu ZQ, An SQ, Miralles DG, Maes W, Liu YL, Tang JW (2018). Potential of solar-induced chlorophyll fluorescence to estimate transpiration in a temperate forest. *Agricultural and Forest Meteorology,* 252, 75-87.

Ma KP (1993). On the concept of biodiversity. *Chinese Biodiversity,* 1, 20-22. [马克平 (1993). 试论生物多样性的概念. 生物多样性, 1, 20-22.]

Ma Y, Liu LY, Chen RN, Du SS, Liu XJ (2020). Generation of a global spatially continuous TanSat solar-induced chlorophyll fluorescence product by considering the impact of the solar radiation intensity. *Remote Sensing,* 12, 2167. DOI: 10.3390/rs12132167.

Ma Y, Liu LY, Liu XJ, Chen JD (2022). An improved downscaled sun-induced chlorophyll fluorescence (DSIF) product of GOME-2 dataset. *European Journal of Remote Sensing,* 55, 168-180.

MacArthur A, Robinson I, Rossini M, Davis N, MacDonald K (2014). A dual-field-of-view spectrometer system for reflectance and fluorescence measurements (Piccolo Doppio) and correction of etaloning//ESA. *Fifth International Workshop on Remote Sensing of Vegetation Fluorescence*. European Space Agenccy, Paris, France.

Maes WH, Pagán BR, Martens B, Gentine P, Guanter L, Steppe K, Verhoest NEC, Dorigo W, Li X, Xiao JF, Miralles DG (2020). Sun-induced fluorescence closely linked to ecosystem transpiration as evidenced by satellite data and radiative transfer models. *Remote Sensing of Environment,* 249, 112030. DOI: 10.1016/j.rse.2020.112030.

Magney TS, Barnes ML, Xi Y (2020). On the covariation of chlorophyll fluorescence and photosynthesis across scales. *Geophysical Research Letters,* 47, e2020GL091098. DOI: 10.1029/2020GL091098.

Magney TS, Bowling DR, Logan BA, Grossmann K, Stutz J, Blanken PD, Burns SP, Cheng R, Garcia MA, Köhler P, Lopez S, Parazoo NC, Raczka B, Schimel D, Frankenberg C (2019). Mechanistic evidence for tracking the seasonality of photosynthesis with solar-induced fluorescence. *Proceedings of the National Academy of Sciences of the United States of America,* 116, 11640-11645.

Maier SW, Günther KP, Stellmes M (2004). Sun-induced fluorescence: a new tool for precision farming. *Digital Imaging and Spectral Techniques*: *Applications to Precision Agriculture,* 66, 209-222.

Marrs JK, Reblin JS, Logan BA, Allen DW, Reinmann AB, Bombard DM, Tabachnik D, Hutyra LR (2020). Solar-induced fluorescence does not track photosynthetic carbon assimilation following induced stomatal closure. *Geophysical Research Letters,* 47, e2020GL087956. DOI: 10.1029/2020gl087956.

Mazzoni M, Meroni M, Fortunato C, Colombo R, Verhoef W (2012). Retrieval of maize canopy fluorescence and reflectance by spectral fitting in the O_2-A absorption band. *Remote Sensing of Environment,* 124, 72-82.

Meng TT, Ni J, Wang GH (2007). Plant functional traits, environments and ecosystem functioning. *Journal of Plant Ecology* (*Chinese Version*), 31, 150-165. [孟婷婷, 倪健, 王国宏 (2007). 植物功能性状与环境和生态系统功能. 植物生态学报, 31, 150-165.]

Meroni M, Barducci A, Cogliati S, Castagnoli F, Rossini M, Busetto L, Migliavacca M, Cremonese E, Galvagno M, Colombo R, di Cella UM (2011). The hyperspectral irradiometer, a new instrument for long-term and unattended field spectroscopy measurements. *Review of Scientific Instruments,* 82, 043106. DOI: 10.1063/1.3574360.

Meroni M, Busetto L, Colombo R, Guanter L, Moreno J, Verhoef W (2010). Performance of spectral fitting methods for vegetation fluorescence quantification. *Remote Sensing of Environment,* 114, 363-374.

Meroni M, Colombo R (2006). Leaf level detection of solar induced chlorophyll fluorescence by means of a subnanometer resolution spectroradiometer. *Remote Sensing of Environment,* 103, 438-448.

Meroni M, Rossini M, Guanter L, Alonso L, Rascher U, Colombo R, Moreno J (2009). Remote sensing of solar-induced chlorophyll fluorescence: review of methods and applications. *Remote Sensing of Environment,* 113, 2037-2051.

Miao G, Guan K, Yang X, Bernacchi C, Berry J, DeLucia E, Wu J, Moore C, Meacham K, Cai YP, Peng B, Kimm H, Masters M (2018). Sun-induced chlorophyll fluorescence, photosynthesis, and light use efficiency of a soybean field from seasonally continuous measurements. *Journal of Geophysical Research: Biogeosciences,* 123, 610-623.

Middleton EM, Huemmrich KF, Zhang Q, Campbell PK, Landis DR (2018). Photosynthetic efficiency and vegetation stress//Thenkabail PS, Lyon JG, Huete A. *Biophysical and Biochemical Characterization and Plant Species Studies*. CRC Press, Boca Raton, USA. 133-179.

Mohammed GH, Colombo R, Middleton EM, Rascher U, van der Tol C, Nedbal L, Goulas Y, Pérez-Priego O, Damm A, Meroni M, Joiner J, Cogliati S, Verhoef W, Malenovský Z, Gastellu-Etchegorry JP, *et al.* (2019). Remote sensing of solar-induced chlorophyll fluorescence (SIF) in vegetation: 50 years of progress. *Remote Sensing of Environment,* 231, 111177. DOI: 10.1016/j.rse.2019.04.030.

Monteith JL (1972). Solar radiation and productivity in tropical ecosystems. *Journal of Applied Ecology,* 9, 747-766.

Moore B, Crowell SMR, Rayner PJ, Kumer J, O'dell CW, O'Brien D, Utembe S, Polonsky I, Schimel D, Lemen J (2018). The potential of the geostationary carbon cycle observatory (GeoCarb) to provide multi-scale constraints

on the carbon cycle in the americas. *Frontiers in Environmental Science,* 6, 109. DOI: 10.3389/fenvs.2018.00109.

Moya I, Daumard F, Moise N, Ounis A, Goulas Y (2006). First airborne multiwavelength passive chlorophyll fluorescence measurements over La Mancha (Spain) fields//Sobrino JA. *Second Recent Advances in Quantitative Remote Sensing*. Publicacions de la Universitat de València, Torrent, Spain. 820-825.

Moya I, Loayza H, López ML, Quiroz R, Ounis A, Goulas Y (2019). Canopy chlorophyll fluorescence applied to stress detection using an easy-to-build micro-lidar. *Photosynthesis Research,* 142, 1-15.

Ni ZY, Liu ZG, Li ZL, Nerry F, Huo HY, Sun R, Yang PQ, Zhang WW (2016). Investigation of atmospheric effects on retrieval of sun-induced fluorescence using hyperspectral imagery. *Sensors,* 16, 480. DOI: 10.3390/s16040480.

Nichol C, Drolet G, Porcar-Castell A, Wade T, Sabater N, Middleton E, MacLellan C, Levula J, Mammarella I, Vesala T, Atherton J (2019). Diurnal and seasonal solar induced chlorophyll fluorescence and photosynthesis in a boreal Scots pine canopy. *Remote Sensing,* 11, 273. DOI: 10.3390/rs11030273.

Odum EP, Barrett GW (1971). *Fundamentals of Ecology*. Saunders, Philadelphia, USA.

Pacheco-Labrador J, Hueni A, Mihai L, Sakowska K, Julitta T, Kuusk J, Sporea D, Alonso L, Burkart A, Mateo MC, Aasen H, Goulas Y, Arthur A (2019). Sun-induced chlorophyll fluorescence I: instrumental considerations for proximal spectroradiometers. *Remote Sensing,* 11, 960. DOI: 10.3390/rs11080960.

Pagán B, Maes W, Gentine P, Martens B, Miralles D (2019). Exploring the potential of satellite solar-induced fluorescence to constrain global transpiration estimates. *Remote Sensing,* 11, 413. DOI: 10.3390/rs11040413.

Paynter I, Cook B, Corp L, Nagol J, McCorkel J (2020). Characterization of FIREFLY, an imaging spectrometer designed for remote sensing of solar induced fluorescence. *Sensors,* 20, 4682. DOI: 10.3390/s20174682.

Peng YJ, Fan J, Xing SH, Cui GF (2018). Overview and classification outlook of natural protected areas in China's mainland. *Biodiversity Science,* 26, 315-325. [彭杨靖, 樊简, 邢韶华, 崔国发 (2018). 中国大陆自然保护地概况及分类体系构想. 生物多样性, 26, 315-325.]

Perez-Priego O, Zarco-Tejada PJ, Miller JR, Sepulcre-Canto G, Fereres E (2005). Detection of water stress in orchard trees with a high-resolution spectrometer through chlorophyll fluorescence in-filling of the O_2-A band. *IEEE Transactions on Geoscience and Remote Sensing,* 43, 2860-2869.

Peterson RB, Oja V, Eichelmann H, Bichele I, Dall'Osto L, Laisk A (2014). Fluorescence F_0 of photosystems II and I in developing C_3 and C_4 leaves, and implications on regulation of excitation balance. *Photosynthesis Research,* 122, 41-56.

Pierrat Z, Magney T, Parazoo NC, Grossmann K, Bowling DR, Seibt U, Johnson B, Helgason W, Barr A, Bortnik J, Norton A, Maguire A, Frankenberg C, Stutz J (2022). Diurnal and seasonal dynamics of solar-induced chlorophyll fluorescence, vegetation indices, and gross primary productivity in the boreal forest. *Journal of Geophysical Research*: *Biogeosciences,* 127, e2021JG006588. DOI: 10.1029/2021jg006588.

Pinto F, Celesti M, Acebron K, Alberti G, Cogliati S, Colombo R, Juszczak R, Matsubara S, Miglietta F, Palombo A, Panigada C, Pignatti S, Rossini M, Sakowska K, Schickling A, *et al.* (2020). Dynamics of Sun-induced chlorophyll fluorescence and reflectance to detect stress-induced variations in canopy photosynthesis. *Plant, Cell & Environment,* 43, 1637-1654.

Pinto F, Damm A, Schickling A, Panigada C, Cogliati S, Müller-Linow M, Balvora A, Rascher U (2016). Sun-induced chlorophyll fluorescence from high-resolution imaging spectroscopy data to quantify spatio-temporal patterns of photosynthetic function in crop canopies. *Plant, Cell & Environment,* 39, 1500-1512.

Plascyk JA (1975). The MK II Fraunhofer line discriminator (FLD-II) for airborne and orbital remote sensing of solar-stimulated luminescence. *Optical Engineering,* 14, 339-346.

Platt U, Stutz J (2008). Differential absorption spectroscopy// Physics Editorial Department. *Physics of Earth and Space Environments.* Springer, Berlin. 135-174.

Porcar-Castell A, Malenovský Z, Magney T, van Wittenberghe S, Fernández-Marín B, Maignan F, Zhang YG, Maseyk K, Atherton J, Albert LP, Robson TM, Zhao F, Garcia-Plazaola JI, Ensminger I, Rajewicz PA, *et al.* (2021). Chlorophyll a fluorescence illuminates a path connecting plant molecular biology to Earth-system science. *Nature Plants,* 7, 998-1009.

Porcar-Castell A, Tyystjärvi E, Atherton J, van der Tol C, Flexas J, Pfündel EE, Moreno J, Frankenberg C, Berry JA (2014). Linking chlorophyll a fluorescence to photosynthesis for remote sensing applications: mechanisms and challenges. *Journal of Experimental Botany,* 65, 4065-4095.

Qin QM, Chen J, Zhang YG, Ren HZ, Wu ZH, Zhang CS, Wu LS, Liu JL (2020). A discussion on some frontier directions of quantitative remote sensing. *Remote Sensing for Land & Resources,* 32, 8-15. [秦其明, 陈晋, 张永光, 任华忠, 吴自华, 张赤山, 吴霖升, 刘见礼 (2020). 定量遥感若干前沿方向探讨. 国土资源遥感, 32, 8-15.]

Qin YW, Xiao XM, Wigneron JP, Ciais P, Canadell JG, Brandt

M, Li XJ, Fan L, Wu XC, Tang H, Dubayah R, Doughty R, Crowell S, Zheng B, Moore B III (2022). Large loss and rapid recovery of vegetation cover and aboveground biomass over forest areas in Australia during 2019–2020. *Remote Sensing of Environment,* 278, 113087. DOI: 10.1016/j.rse.2022.113087.

Qiu B, Chen JM, Ju WM, Zhang Q, Zhang YG (2019). Simulating emission and scattering of solar-induced chlorophyll fluorescence at far-red band in global vegetation with different canopy structures. *Remote Sensing of Environment,* 233, 111373. DOI: 10.1016/j.rse.2019.111373.

Qiu B, Ge J, Guo WD, Pitman AJ, Mu MY (2020). Responses of Australian dryland vegetation to the 2019 heat wave at a subdaily scale. *Geophysical Research Letters,* 47, e2019GL086569. DOI: 10.1029/2019gl086569.

Qiu RN, Li X, Han G, Xiao JF, Ma X, Gong W (2022). Monitoring drought impacts on crop productivity of the US Midwest with solar-induced fluorescence: GOSIF outperforms GOME-2 SIF and MODIS NDVI, EVI, and NIRv. *Agricultural and Forest Meteorology,* 323, 109038. DOI: 10.1016/j.agrformet.2022.109038.

Rascher U, Alonso L, Burkart A, Cilia C, Cogliati S, Colombo R, Damm A, Drusch M, Guanter L, Hanus J, Hyvärinen T, Julitta T, Jussila J, Kataja K, Kokkalis P, *et al.* (2015). Sun-induced fluorescence—A new probe of photosynthesis: first maps from the imaging spectrometer HyPlant. *Global Change Biology,* 21, 4673-4684.

Rietkerk M, van de Koppel J (2008). Regular pattern formation in real ecosystems. *Trends in Ecology & Evolution,* 23, 169-175.

Rigden AJ, Salvucci GD, Entekhabi D, Short Gianotti DJ (2018). Partitioning evapotranspiration over the continental United States using weather station data. *Geophysical Research Letters,* 45, 9605-9613.

Rossini M, Nedbal L, Guanter L, Ač A, Alonso L, Burkart A, Cogliati S, Colombo R, Damm A, Drusch M, Hanus J, Janoutova R, Julitta T, Kokkalis P, Moreno J, *et al.* (2015a). Red and far red sun-induced chlorophyll fluorescence as a measure of plant photosynthesis. *Geophysical Research Letters,* 42, 1632-1639.

Rossini M, Panigada C, Cilia C, Meroni M, Busetto L, Cogliati S, Amaducci S, Colombo R (2015b). Discriminating irrigated and rainfed maize with diurnal fluorescence and canopy temperature airborne maps. *ISPRS International Journal of Geo-Information,* 4, 626-646.

Ryu Y, Berry JA, Baldocchi DD (2019). What is global photosynthesis? History, uncertainties and opportunities. *Remote Sensing of Environment,* 223, 95-114.

Schlesinger WH, Jasechko S (2014). Transpiration in the global water cycle. *Agricultural and Forest Meteorology,* 189-190, 115-117.

Schreiber U, Schliwa U, Bilger W (1986). Continuous recording of photochemical and non-photochemical chlorophyll fluorescence quenching with a new type of modulation fluorometer. *Photosynthesis Research,* 10, 51-62.

Shan N, Ju WM, Migliavacca M, Martini D, Guanter L, Chen JM, Goulas Y, Zhang YG (2019). Modeling canopy conductance and transpiration from solar-induced chlorophyll fluorescence. *Agricultural and Forest Meteorology,* 268, 189-201.

Shan N, Zhang YG, Chen JM, Ju WM, Migliavacca M, Peñuelas J, Yang X, Zhang ZY, Nelson JA, Goulas Y (2021). A model for estimating transpiration from remotely sensed solar-induced chlorophyll fluorescence. *Remote Sensing of Environment,* 252, 112134. DOI: 10.1016/j.rse.2020.112134.

Shi GY, Huang H, Sang YQ, Cai LL, Zhang JS, Cheng XF, Meng P, Sun SJ, Li JX, Qiao YS (2022). Solar-induced chlorophyll fluorescence intensity has a significant correlation with negative air ion release in forest canopy. *Atmospheric Environment,* 269, 118873. DOI: 10.1016/j.atmosenv.2021.118873.

Smith WK, Biederman JA, Scott RL, Moore DJP, He M, Kimball JS, Yan D, Hudson A, Barnes ML, MacBean N, Fox AM, Litvak ME (2018). Chlorophyll fluorescence better captures seasonal and interannual gross primary productivity dynamics across dryland ecosystems of southwestern north America. *Geophysical Research Letters,* 45, 748-757.

Smith WK, Dannenberg MP, Yan D, Herrmann S, Barnes ML, Barron-Gafford GA, Biederman JA, Ferrenberg S, Fox AM, Hudson A, Knowles JF, MacBean N, Moore DJP, Nagler PL, Reed SC, *et al.* (2019). Remote sensing of dryland ecosystem structure and function: progress, challenges, and opportunities. *Remote Sensing of Environment,* 233, 111401. DOI: 10.1016/j.rse.2019.111401.

Song L, Guanter L, Guan KY, You LZ, Huete A, Ju WM, Zhang YG (2018). Satellite sun-induced chlorophyll fluorescence detects early response of winter wheat to heat stress in the Indian Indo-Gangetic Plains. *Global Change Biology,* 24, 4023-4037.

Song Y, Wang J, Wang LX (2020). Satellite solar-induced chlorophyll fluorescence reveals heat stress impacts on wheat yield in *India*. *Remote Sensing,* 12, 3277. DOI: 10.3390/rs12203277.

Stoy P, El-Madany T, Fisher J, Gentine P, Gerken T, Good S, Klosterhalfen A, Liu SG, Miralles D, Pérez-Priego Ó, Rigden A, Skaggs T, Wohlfahrt G, Anderson R, Coenders-Gerrits A, *et al.* (2019). Reviews and syntheses: turning the challenges of partitioning ecosystem evaporation and transpiration into opportunities. *Biogeosciences,* 16,

3747-3775.

Su YJ, Wu FF, Ao ZR, Jin SC, Qin F, Liu BX, Pang SX, Liu LL, Guo QH (2019). Evaluating maize phenotype dynamics under drought stress using terrestrial lidar. *Plant Methods,* 15, 1-16.

Sun Y, Frankenberg C, Jung M, Joiner J, Guanter L, Köhler P, Magney T (2018). Overview of solar-induced chlorophyll fluorescence (SIF) from the Orbiting Carbon Observatory-2: retrieval, cross-mission comparison, and global monitoring for GPP. *Remote Sensing of Environment,* 209, 808-823.

Sun Y, Frankenberg C, Wood JD, Schimel DS, Jung M, Guanter L, Drewry DT, Verma M, Porcar-Castell A, Griffis TJ, Gu L, Magney TS, Köhler P, Evans B, Yuen K (2017). OCO-2 advances photosynthesis observation from space via solar-induced chlorophyll fluorescence. *Science,* 358, eaam5747. DOI: 10.1126/science.aam5747.

Sun Y, Fu R, Dickinson R, Joiner J, Frankenberg C, Gu LH, Xia YL, Fernando N (2015). Drought onset mechanisms revealed by satellite solar-induced chlorophyll fluorescence: insights from two contrasting extreme events. *Journal of Geophysical Research: Biogeosciences,* 120, 2427-2440.

Tagliabue G, Panigada C, Celesti M, Cogliati S, Colombo R, Migliavacca M, Rascher U, Rocchini D, Schüttemeyer D, Rossini M (2020). Sun-induced fluorescence heterogeneity as a measure of functional diversity. *Remote Sensing of Environment,* 247, 111934. DOI: 10.1016/j.rse.2020.111934.

Taiz L, Zeiger E, Møller IM, Murphy A (2015). *Plant Physiology and Development.* Sinauer Associates Incorporated, Sunderland, USA.

Tang XG, Xiao JF, Ma MG, Yang H, Li X, Ding Z, Yu PJ, Zhang YG, Wu CY, Huang J, Thompson JR (2022). Satellite evidence for China's leading role in restoring vegetation productivity over global karst ecosystems. *Forest Ecology and Management,* 507, 120000. DOI: 10.1016/j.foreco.2021.120000.

Taylor TE, Eldering A, Merrelli A, Kiel M, Somkuti P, Cheng C, Rosenberg R, Fisher B, Crisp D, Basilio R, Bennett M, Cervantes D, Chang A, Dang L, Frankenberg C, *et al.* (2020). OCO-3 early mission operations and initial (vEarly) XCO_2 and SIF retrievals. *Remote Sensing of Environment,* 251, 112032. DOI: 10.1016/j.rse.2020.112032.

Tubuxin B, Rahimzadeh-Bajgiran P, Ginnan Y, Hosoi F, Omasa K (2015). Estimating chlorophyll content and photochemical yield of photosystem II (ΦPSII) using solar-induced chlorophyll fluorescence measurements at different growing stages of attached leaves. *Journal of Experimental Botany,* 66, 5595-5603.

van der Tol C, Rossini M, Cogliati S, Verhoef W, Colombo R, Rascher U, Mohammed G (2016). A model and measurement comparison of diurnal cycles of sun-induced chlorophyll fluorescence of crops. *Remote Sensing of Environment,* 186, 663-677.

van der Tol C, Verhoef W, Timmermans J, Verhoef A, Su Z (2009). An integrated model of soil-canopy spectral radiances, photosynthesis, fluorescence, temperature and energy balance. *Biogeosciences,* 6, 3109-3129.

Verrelst J, Rivera JP, van der Tol C, Magnani F, Mohammed G, Moreno J (2015). Global sensitivity analysis of the SCOPE model: What drives simulated canopy-leaving sun-induced fluorescence? *Remote Sensing of Environment,* 166, 8-21.

von Hebel C, Matveeva M, Verweij E, Rademske P, Kaufmann M, Brogi C, Vereecken H, Rascher U, van der Kruk J (2018). Understanding soil and plant interaction by combining ground-based quantitative electromagnetic induction and airborne hyperspectral data. *Geophysical Research Letters,* 45, 7571-7579.

Walther S, Voigt M, Thum T, Gonsamo A, Zhang YG, Köhler P, Jung M, Varlagin A, Guanter L (2016). Satellite chlorophyll fluorescence measurements reveal large-scale decoupling of photosynthesis and greenness dynamics in boreal evergreen forests. *Global Change Biology,* 22, 2979-2996.

Wang C, Beringer J, Hutley L, Cleverly J, Li J, Liu QH, Sun Y (2019a). Phenology dynamics of dryland ecosystems along the north Australian tropical transect revealed by satellite solar-induced chlorophyll fluorescence. *Geophysical Research Letters,* 46, 5294-5302.

Wang J, Zhong XM, Lv XL, Shi ZS, Li FH (2018). Photosynthesis and physiology responses of paired near-isogenic lines in waxy maize (*Zea mays* L.) to nicosulfuron. *Photosynthetica,* 56, 1059-1068.

Wang MY, Luo Y, Zhang ZY, Xie QY, Wu XD, Ma XL (2022). Recent advances in remote sensing of vegetation phenology: retrieval algorithm and validation strategy. *National Remote Sensing Bulletin,* 26, 431-455. [王敏钰, 罗毅, 张正阳, 谢巧云, 吴小丹, 马轩龙 (2022). 植被物候参数遥感提取与验证方法研究进展. 遥感学报, 26, 431-455.]

Wang N, Suomalainen J, Bartholomeus H, Kooistra L, Masiliūnas D, Clevers JGPW (2021). Diurnal variation of Sun-induced chlorophyll fluorescence of agricultural crops observed from a point-based spectrometer on a UAV. *International Journal of Applied Earth Observation and Geoinformation,* 96, 102276. DOI: 10.1016/j.jag.2020.102276.

Wang SH, Huang CP, Zhang LF, Gao XL, Fu AM (2019). Designment and assessment of far-red solar-induced chlorophyll fluorescence retrieval method for the terrestrial ecosystem carbon inventory satellite. *Remote Sensing Technology and Application,* 34, 476-487. [王思恒, 黄长平, 张立福, 高显连, 付安民 (2019). 陆地生

DOI: 10.17521/cjpe.2022.0233

态系统碳监测卫星远红波段叶绿素荧光反演算法设计. 遥感技术与应用, 34, 476-487.]

Wang SH, Ju WM, Peñuelas J, Cescatti A, Zhou YY, Fu YS, Huete A, Liu M, Zhang YG (2019b). Urban-rural gradients reveal joint control of elevated CO_2 and temperature on extended photosynthetic seasons. *Nature Ecology & Evolution,* 3, 1076-1085.

Wang SH, Zhang YG, Ju W, Chen J, Ciais P, Cescatti A, Sardans J, Janssens I, Wu MS, Berry J, Campbell E, Fernández-Martínez M, Alkama R, Sitch S, Friedlingstein P, *et al.* (2020). Recent global decline of CO_2 fertilization effects on vegetation photosynthesis. *Science,* 370, 1295-1300.

Wang X, Biederman JA, Knowles JF, Scott RL, Turner AJ, Dannenberg MP, Köhler P, Frankenberg C, Litvak ME, Flerchinger GN, Law BE, Kwon H, Reed SC, Parton WJ, Barron-Gafford GA, Smith WK (2022). Satellite solar-induced chlorophyll fluorescence and near-infrared reflectance capture complementary aspects of dryland vegetation productivity dynamics. *Remote Sensing of Environment,* 270, 112858. DOI: 10.1016/j.rse.2021.112858.

Wang XR, Qiu B, Li WK, Zhang Q (2019c). Impacts of drought and heatwave on the terrestrial ecosystem in China as revealed by satellite solar-induced chlorophyll fluorescence. *Science of the Total Environment,* 693, 133627. DOI: 10.1016/j.scitotenv.2019.133627.

Wang YJ, Frankenberg C (2022). On the impact of canopy model complexity on simulated carbon, water, and solar-induced chlorophyll fluorescence fluxes. *Biogeosciences,* 19, 29-45.

Wen J, Köhler P, Duveiller G, Parazoo NC, Magney TS, Hooker G, Yu L, Chang CY, Sun Y (2020). A framework for harmonizing multiple satellite instruments to generate a long-term global high spatial-resolution solar-induced chlorophyll fluorescence (SIF). *Remote Sensing of Environment,* 239, 111644. DOI: 10.1016/j.rse.2020.111644.

Wieneke S, Ahrends H, Damm A, Pinto F, Stadler A, Rossini M, Rascher U (2016). Airborne based spectroscopy of red and far-red sun-induced chlorophyll fluorescence: implications for improved estimates of gross primary productivity. *Remote Sensing of Environment,* 184, 654-667.

Wieneke S, Burkart A, Cendrero-Mateo MP, Julitta T, Rossini M, Schickling A, Schmidt M, Rascher U (2018). Linking photosynthesis and sun-induced fluorescence at sub-daily to seasonal scales. *Remote Sensing of Environment,* 219, 247-258.

Wolanin A, Rozanov VV, Dinter T, Noël S, Vountas M, Burrows JP, Bracher A (2015). Global retrieval of marine and terrestrial chlorophyll fluorescence at its red peak using hyperspectral top of atmosphere radiance measurements: feasibility study and first results. *Remote Sensing of Environment,* 166, 243-261.

Wu JP, Su YX, Chen XZ, Liu LY, Yang XQ, Gong FX, Zhang HO, Xiong X, Zhang DQ (2021). Leaf shedding of Pan-Asian tropical evergreen forests depends on the synchrony of seasonal variations of rainfall and incoming solar radiation. *Agricultural and Forest Meteorology,* 311, 108691. DOI: 10.1016/j.agrformet.2021.108691.

Wu LS, Wang L, Shi C, Yin DM (2022a). Detecting mangrove photosynthesis with solar-induced chlorophyll fluorescence. *International Journal of Remote Sensing,* 43, 1037-1053.

Wu LS, Zhang XK, Rossini M, Wu YF, Zhang ZY, Zhang YG (2022b). Physiological dynamics dominate the response of canopy far-red solar-induced fluorescence to herbicide treatment. *Agricultural and Forest Meteorology,* 323, 109063. DOI: 10.1016/j.agrformet.2022.109063.

Xia JY, Lu RL, Zhu C, Cui EQ, Du Y, Huang K, Sun BY (2020). Response and adaptation of terrestrial ecosystem processes to climate warming. *Chinese Journal of Plant Ecology,* 44, 494-514. [夏建阳, 鲁芮伶, 朱辰, 崔二乾, 杜莹, 黄昆, 孙宝玉 (2020). 陆地生态系统过程对气候变暖的响应与适应. 植物生态学报, 44, 494-514.]

Xiao JF, Fisher JB, Hashimoto H, Ichii K, Parazoo NC (2021). Emerging satellite observations for diurnal cycling of ecosystem processes. *Nature Plants,* 7, 877-887.

Xie XM, He B, Guo LL, Huang L, Hao XM, Zhang YF, Liu XB, Tang R, Wang SF (2022). Revisiting dry season vegetation dynamics in the Amazon rainforest using different satellite vegetation datasets. *Agricultural and Forest Meteorology,* 312, 108704. DOI: 10.1016/j.agrformet.2021.108704.

Xu S, Atherton J, Riikonen A, Zhang C, Oivukkamäki J, MacArthur A, Honkavaara E, Hakala T, Koivumäki N, Liu ZG, Porcar-Castell A (2021). Structural and photosynthetic dynamics mediate the response of SIF to water stress in a potato crop. *Remote Sensing of Environment,* 263, 112555. DOI: 10.1016/j.rse.2021.112555.

Xu S, Liu ZG, Zhao L, Zhao HR, Ren SX (2018). Diurnal response of sun-induced fluorescence and PRI to water stress in maize using a near-surface remote sensing platform. *Remote Sensing,* 10, 1510. DOI: 10.3390/rs10101510.

Yan S, Zhang L, Jing YS, He HL, Yu GR (2014). Variations in the relationship between maximum leaf carboxylation rate and leaf nitrogen concentration. *Chinese Journal of Plant Ecology,* 38, 640-652. [闫霜, 张黎, 景元书, 何洪林, 于贵瑞 (2014). 植物叶片最大羧化速率与叶氮含量关系的变异性. 植物生态学报, 38, 640-652.]

Yang JC, Magney T, Albert L, Richardson AD, Frankenberg C, Stutz J, Grossmann K, Burns S, Seyednasrollah B,

Blanken P, Bowling D (2022). Gross primary production (GPP) and red solar induced fluorescence (SIF) respond differently to light and seasonal environmental conditions in a subalpine conifer forest. *Agricultural and Forest Meteorology,* 317, 108904. DOI: 10.1016/j.agrformet.2022.108904.

Yang KG, Ryu Y, Dechant B, Berry JA, Hwang Y, Jiang CY, Kang M, Kim J, Kimm H, Kornfeld A, Yang X (2018a). Sun-induced chlorophyll fluorescence is more strongly related to absorbed light than to photosynthesis at half-hourly resolution in a rice paddy. *Remote Sensing of Environment,* 216, 658-673.

Yang P, van der Tol C, Campbell P, Middleton E (2021). Unraveling the physical and physiological basis for the solar-induced chlorophyll fluorescence and photosynthesis relationship using continuous leaf and canopy measurements of a corn crop. *Biogeosciences,* 18, 441-465.

Yang PQ, van der Tol C (2018). Linking canopy scattering of far-red sun-induced chlorophyll fluorescence with reflectance. *Remote Sensing of Environment,* 209, 456-467.

Yang PQ, van der Tol C, Campbell PKE, Middleton EM (2020). Fluorescence Correction Vegetation Index (FCVI): a physically based reflectance index to separate physiological and non-physiological information in far-red sun-induced chlorophyll fluorescence. *Remote Sensing of Environment,* 240, 111676. DOI: 10.1016/j.rse.2020.111676.

Yang X, Shi HY, Stovall A, Guan KY, Miao GF, Zhang YG, Zhang Y, Xiao XM, Ryu Y, Lee JE (2018b). FluoSpec 2—An automated field spectroscopy system to monitor canopy solar-induced fluorescence. *Sensors,* 18, 2063. DOI: 10.3390/s18072063.

Yang X, Tang JW, Mustard JF, Lee JE, Rossini M, Joiner J, Munger JW, Kornfeld A, Richardson AD (2015). Solar-induced chlorophyll fluorescence that correlates with canopy photosynthesis on diurnal and seasonal scales in a temperate deciduous forest. *Geophysical Research Letters,* 42, 2977-2987.

Yao L, Liu Y, Yang DX, Cai Z, Wang J, Lin C, Lu N, Lyu D, Tian L, Wang MH, Yin Z, Zheng YQ, Wang SS (2022). Retrieval of solar-induced chlorophyll fluorescence (SIF) from satellite measurements: comparison of SIF between TanSat and OCO-2. *Atmospheric Measurement Techniques,* 15, 2125-2137.

Yao L, Yang DX, Liu Y, Wang J, Liu LY, Du SS, Cai ZN, Lu NM, Lyu DR, Wang MH, Yin ZS, Zheng YQ (2021). A new global solar-induced chlorophyll fluorescence (SIF) data product from TanSat measurements. *Advances in Atmospheric Sciences,* 38, 341-345.

Yoshida Y, Joiner J, Tucker C, Berry J, Lee JE, Walker G, Reichle R, Koster R, Lyapustin A, Wang Y (2015). The 2010 Russian drought impact on satellite measurements of solar-induced chlorophyll fluorescence: insights from modeling and comparisons with parameters derived from satellite reflectances. *Remote Sensing of Environment,* 166, 163-177.

Yu GR, Zhang L, He HL, Yang M (2021). A process-based model and simulation system of dynamic change and spatial variation in large-scale terrestrial ecosystems. *Chinese Journal of Applied Ecology,* 32, 2653-2665. [于贵瑞, 张黎, 何洪林, 杨萌 (2021). 大尺度陆地生态系统动态变化与空间变异的过程模型及模拟系统. 应用生态学报, 32, 2653-2665.]

Yu L, Wen J, Chang CY, Frankenberg C, Sun Y (2019). High-resolution global contiguous SIF of OCO-2. *Geophysical Research Letters,* 46, 1449-1458.

Yue YM, Wang KL, Zhang B, Chen ZC (2008). Applications of hyperspectral remote sensing in ecosystem: a review. *Remote Sensing Technology and Application,* 23, 471-478. [岳跃民, 王克林, 张兵, 陈正超 (2008). 高光谱遥感在生态系统研究中的应用进展. 遥感技术与应用, 23, 471-478.]

Zarco-Tajeda PJ, Miller JR, Haboudane D, Tremblay N, Apostol S (2003). Detection of chlorophyll fluorescence in vegetation from airborne hyperspectral CASI imagery in the red edge spectral region//IEEE. *2003 IEEE International Geoscience and Remote Sensing Symposium Proceedings.* IEEE, Toulouse, France. 598-600.

Zarco-Tejada PJ, Berni JAJ, Suárez L, Sepulcre-Cantó G, Morales F, Miller JR (2009). Imaging chlorophyll fluorescence with an airborne narrow-band multispectral camera for vegetation stress detection. *Remote Sensing of Environment,* 113, 1262-1275.

Zarco-Tejada PJ, González-Dugo V, Berni JAJ (2012). Fluorescence, temperature and narrow-band indices acquired from a UAV platform for water stress detection using a micro-hyperspectral imager and a thermal camera. *Remote Sensing of Environment,* 117, 322-337.

Zarco-Tejada PJ, Poblete T, Camino C, Gonzalez-Dugo V, Calderon R, Hornero A, Hernandez-Clemente R, Román-Écija M, Velasco-Amo MP, Landa BB, Beck PSA, Saponari M, Boscia D, Navas-Cortes JA (2021). Divergent abiotic spectral pathways unravel pathogen stress signals across species. *Nature Communications,* 12, 6088. DOI: 10.1038/s41467-021-26335-3.

Zeng YL, Badgley G, Chen M, Li J, Anderegg LDL, Kornfeld A, Liu QH, Xu BD, Yang B, Yan K, Berry JA (2020). A radiative transfer model for solar induced fluorescence using spectral invariants theory. *Remote Sensing of Environment,* 240, 111678. DOI: 10.1016/j.rse.2020.111678.

Zeng YL, Badgley G, Dechant B, Ryu Y, Chen M, Berry JA (2019). A practical approach for estimating the escape ratio of near-infrared solar-induced chlorophyll

fluorescence. *Remote Sensing of Environment,* 232, 111209. DOI: 10.1016/j.rse.2019.05.028.

Zeng YL, Chen M, Hao DL, Damm A, Badgley G, Rascher U, Johnson JE, Dechant B, Siegmann B, Ryu Y, Qiu H, Krieger V, Panigada C, Celesti M, Miglietta F, *et al.* (2022a). Combining near-infrared radiance of vegetation and fluorescence spectroscopy to detect effects of abiotic changes and stresses. *Remote Sensing of Environment,* 270, 112856. DOI: 10.1016/j.rse.2021. 112856.

Zeng YL, Hao DL, Huete A, Dechant B, Berry J, Chen JM, Joiner J, Frankenberg C, Bond-Lamberty B, Ryu Y, Xiao JF, Asrar GR, Chen M (2022b). Optical vegetation indices for monitoring terrestrial ecosystems globally. *Nature Reviews Earth & Environment,* 3, 477-493.

Zhang LF, Qiao N, Huang CP, Wang SH (2019a). Monitoring drought effects on vegetation productivity using satellite solar-induced chlorophyll fluorescence. *Remote Sensing,* 11, 378. DOI: 10.3390/rs11040378.

Zhang XK, Zhang ZY, Zhang YG, Zhang Q, Liu XJ, Chen JD, Wu YF, Wu LS (2022a). Influences of fractional vegetation cover on the spatial variability of canopy SIF from unmanned aerial vehicle observations. *International Journal of Applied Earth Observation and Geoinformation,* 107, 102712. DOI: 10.1016/j.jag.2022. 102712.

Zhang Y, Joiner J, Alemohammad SH, Zhou S, Gentine P (2018a). A global spatially contiguous solar-induced fluorescence (CSIF) dataset using neural networks. *Biogeosciences,* 15, 5779-5800.

Zhang Y, Xiao XM, Wolf S, Wu JY, Wu XC, Gioli B, Wohlfahrt G, Cescatti A, Tol C, Zhou S, Gough C, Gentine P, Zhang YG, Steinbrecher R, Ardö J (2018b). Spatio-temporal convergence of maximum daily light-use efficiency based on radiation absorption by canopy chlorophyll. *Geophysical Research Letters,* 45, 3508-3519.

Zhang YG, Guanter L, Berry JA, Joiner J, van der Tol C, Huete A, Gitelson A, Voigt M, Köhler P (2014). Estimation of vegetation photosynthetic capacity from space-based measurements of chlorophyll fluorescence for terrestrial biosphere models. *Global Change Biology,* 20, 3727-3742.

Zhang YG, Guanter L, Berry JA, van der Tol C, Yang X, Tang JW, Zhang FM (2016). Model-based analysis of the relationship between Sun-induced chlorophyll fluorescence and gross primary production for remote sensing applications. *Remote Sensing of Environment,* 187, 145-155.

Zhang YG, Guanter L, Joiner J, Song L, Guan KY (2018c). Spatially-explicit monitoring of crop photosynthetic capacity through the use of space-based chlorophyll fluorescence data. *Remote Sensing of Environment,* 210, 362-374.

Zhang YG, Zhang Q, Liu LY, Zhang YJ, Wang SQ, Ju WM, Zhou GS, Zhou L, Tang JW, Zhu XD, Wang F, Huang Y, Zhang ZZ, Qiu B, Zhang XK, *et al.* (2021a). ChinaSpec: a network for long-term ground-based measurements of solar-induced fluorescence in China. *Journal of Geophysical Research: Biogeosciences,* 126, e2020JG006042. DOI: 10.1029/2020jg006042.

Zhang YJ, Fan CK, Huang K, Liu YJ, Zu JX, Zhu JT (2017). Opportunities and challenges in remote sensing applications to ecosystem ecology. *Chinese Journal of Ecology,* 36, 809-823. [张扬建, 范春捆, 黄珂, 刘瑶杰, 俎佳星, 朱军涛 (2017). 遥感在生态系统生态学上应用的机遇与挑战. 生态学杂志, 36, 809-823.]

Zhang YM, Zhou GS (2012). Advances in leaf maximum carboxylation rate and its response to environmental factors. *Acta Ecologica Sinica,* 32, 5907-5917. [张彦敏, 周广胜 (2012). 植物叶片最大羧化速率及其对环境因子响应的研究进展. 生态学报, 32, 5907-5917.]

Zhang ZX, Xu W, Qin QM, Chen YJ (2020a). Monitoring and assessment of agricultural drought based on solar-induced chlorophyll fluorescence during growing season in North China Plain. *IEEE Journal of Selected Topics in Applied Earth Observations and Remote Sensing,* 14, 775-790.

Zhang ZY, Wang SH, Qiu B, Song L, Zhang YG (2019). Retrieval of sun-induced chlorophyll fluorescence and advancements in carbon cycle application. *Journal of Remote Sensing,* 23, 37-52. [章钊颖, 王松寒, 邱博, 宋练, 张永光 (2019). 日光诱导叶绿素荧光遥感反演及碳循环应用进展. 遥感学报, 23, 37-52.]

Zhang ZY, Zhang XK, Albert PC, Chen JM, Ju WM, Wu LS, Wu YF, Zhang YG (2022b). Sun-induced chlorophyll fluorescence is more strongly related to photosynthesis with hemispherical than nadir measurements: evidence from field observations and model simulations. *Remote Sensing of Environment,* 279, 113118. DOI: 10.1016/j.rse.2022.113118.

Zhang ZY, Zhang YG, Joiner J, Migliavacca M (2018d). Angle matters: Bidirectional effects impact the slope of relationship between gross primary productivity and sun-induced chlorophyll fluorescence from Orbiting Carbon Observatory-2 across biomes. *Global Change Biology,* 24, 5017-5020.

Zhang ZY, Zhang YG, Porcar-Castell A, Joiner J, Guanter L, Yang X, Migliavacca M, Ju WM, Sun ZG, Chen SP, Martini D, Zhang Q, Li ZH, Cleverly J, Wang HZ, Goulas Y (2020b). Reduction of structural impacts and distinction of photosynthetic pathways in a global estimation of GPP from space-borne solar-induced chlorophyll fluorescence. *Remote Sensing of Environment,* 240, 111722. DOI: 10.1016/j.rse.2020.111722.

Zhang ZY, Zhang YG, Zhang Q, Chen JM, Porcar-Castell A, Guanter L, Wu YF, Zhang XK, Wang HZ, Ding DW, Li ZY (2020c). Assessing bi-directional effects on the diurnal

cycle of measured solar-induced chlorophyll fluorescence in crop canopies. *Agricultural and Forest Meteorology,* 295, 108147. DOI: 10.1016/j.agrformet.2020.108147.

Zhang ZZ, Chen JM, Guanter L, He LM, Zhang YG (2019b). From canopy-leaving to total canopy far-red fluorescence emission for remote sensing of photosynthesis: first results from TROPOMI. *Geophysical Research Letters,* 46, 12030-12040.

Zhang ZZ, Zhang YG, Chen JM, Ju WM, Migliavacca M, El-Madany TS (2021b). Sensitivity of estimated total canopy SIF emission to eemotely sensed LAI and BRDF products. *Journal of Remote Sensing,* 1, 145-162.

Zhang, Zhang, Li, Wu, Zhang (2019c). Comparison of Bi-hemispherical and hemispherical-conical configurations for *in situ* measurements of solar-induced chlorophyll fluorescence. *Remote Sensing,* 11, 2642. DOI: 10.3390/rs11222642.

Zhao DY, Hou YQ, Zhang ZY, Wu YF, Zhang XK, Wu LS, Zhu XL, Zhang YG (2022a). Temporal resolution of vegetation indices and solar-induced chlorophyll fluorescence data affects the accuracy of vegetation phenology estimation: a study using *in situ* measurements. *Ecological Indicators,* 136, 108673. DOI: 10.1016/j.ecolind.2022.108673.

Zhao F, Guo YQ, Verhoef W, Gu XF, Liu LY, Yang GJ (2014). A method to reconstruct the solar-induced canopy fluorescence spectrum from hyperspectral measurements. *Remote Sensing,* 6, 10171-10192.

Zhao F, Li R, Verhoef W, Cogliati S, Liu XJ, Huang YB, Guo YQ, Huang JX (2018). Reconstruction of the full spectrum of solar-induced chlorophyll fluorescence: intercomparison study for a novel method. *Remote Sensing of Environment,* 219, 233-246.

Zhao F, Li ZJ, Verhoef W, Fan CR, Luan HX, Yin TG, Zhang J, Liu ZQ, Tong CM, Bao YF (2022b). Simulation of solar-induced chlorophyll fluorescence by modeling radiative coupling between vegetation and atmosphere with WPS. *Remote Sensing of Environment,* 277, 113075. DOI: 10.1016/j.rse.2022.113075.

Zheng SX, Shangguan ZP (2007). Photosynthetic characteristics and their relationships with leaf nitrogen content and leaf mass per area in different plant functional types. *Acta Ecologica Sinica,* 27, 171-181. [郑淑霞, 上官周平 (2007). 不同功能型植物光合特性及其与叶氮含量、比叶重的关系. 生态学报, 27, 171-181.]

Zhou L, Chi YG, Liu XT, Dai XQ, Yang FT (2020). Land surface phenology tracked by remotely sensed sun-induced chlorophyll fluorescence in subtropical evergreen coniferous forests. *Acta Ecologica Sinica,* 40, 4114-4125. [周蕾, 迟永刚, 刘啸添, 戴晓琴, 杨风亭 (2020). 日光诱导叶绿素荧光对亚热带常绿针叶林物候的追踪. 生态学报, 40, 4114-4125.]

Zhou YY (2022). Understanding urban plant phenology for sustainable cities and planet. *Nature Climate Change,* 12, 302-304.

Zhu XD, Hou YW, Zhang YG, Lu XL, Liu ZQ, Weng QH (2021). Potential of Sun-induced chlorophyll fluorescence for indicating mangrove canopy photosynthesis. *Journal of Geophysical Research*: *Biogeosciences,* 126, e2020JG006159. DOI: 10.1029/2020jg006159.

责任编委: 苏艳军 责任编辑: 李 敏

DOI: 10.17521/cjpe.2022.0233